INL/EXT-12-24617
Revision 0

# Thermodynamic Assessment of Hot Corrosion Mechanisms of Superalloys Hastelloy N and Haynes 242 in Eutectic Mixture of Molten Salts KF and $ZrF_4$

Michael V. Glazoff

February 2012

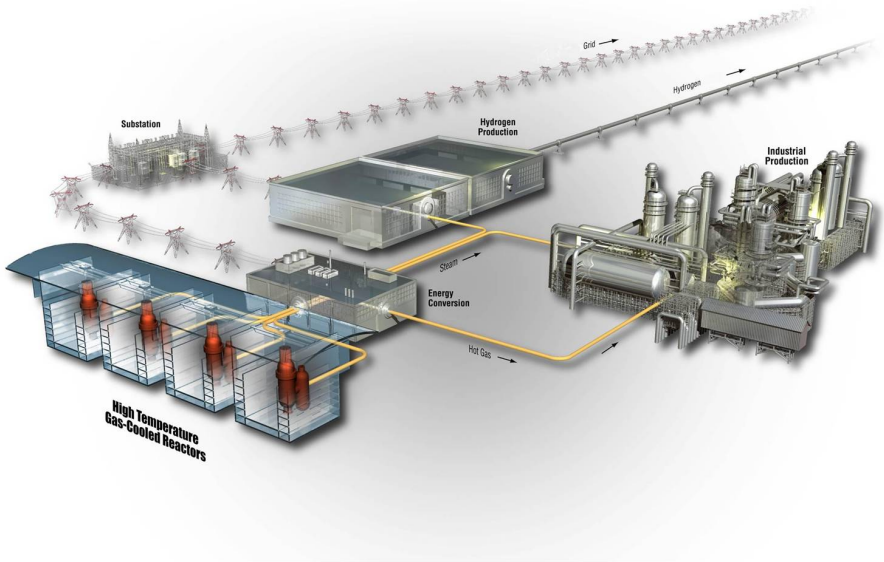


The INL is a
U.S. Department of Energy
National Laboratory
operated by
Battelle Energy Alliance

Idaho National Laboratory

INL/EXT-12-24617
Revision 0

# Thermodynamic Assessment of Hot Corrosion Mechanisms of Superalloys Hastelloy N and Haynes 242 in Eutectic Mixture of Molten Salts KF and ZrF4

Michael V. Glazoff

February 2012

Idaho National Laboratory
Idaho Falls, Idaho 83415

Prepared for the
U.S. Department of Energy
Office of Nuclear Energy
Under DOE Idaho Operations Office
Contract DE-AC07-05ID14517

# Thermodynamic Assessment of Hot Corrosion Mechanisms of Superalloys Hastelloy N and Haynes 242 in Eutectic Mixture of Molten Salts KF and $ZrF_4$

**INL/EXT-12-24617**
**Revision 0**

**February 2012**

**Approved by:**

M. V. Glazoff
Author

02/16/2012
Date

M. G. McKellar
Project Technical Lead

16 Feb 2012
Date

# ABSTRACT

This computational work models the behavior of Haynes 242 and Hastelloy N in the binary molten salt eutectic mixture KF-$ZrF_4$. Limiting the principal alloying elements to four—nickel, chromium, molybdenum, and iron—allows reasonable conclusions to be made about the nature of the hot corrosion resistance of these materials. It suggests that alloy composition optimization work could be conducted to further enhance alloy hot corrosion resistance.

The onset of hot corrosion for both alloys is associated with chromium leaching and the formation of $CrF_2$ in relatively mild oxidizing conditions. However, the onset of hot corrosion for Alloy N requires harsher conditions than for Haynes 242. Thermodynamic data for these systems need to be generated in future research efforts in order to get a clearer picture of the mechanisms of hot corrosion onset. First-principles atomistic simulations can illuminate those cases where experimental thermodynamic data is absent.

Another important direction of research is coupling, in real time, the hydrodynamics of molten salt flow inside the reactor with a thermodynamic assessment of corrosion made under the assumption of local equilibrium on a sufficiently fine spatio-temporal grid. This would pave the way to understanding how corrosion develops in real space and time in heat exchanger loop components made of superalloys and steels. A possible application of this new technology would be the analysis of pyrolytic processes, when molten salts are used for catalytic purposes (e.g., biomass reactors, obtaining quality fuel out of heavy fractions of oil refining, etc.).

Continuing this computational research effort will allow nuclear engineers to approach the problem of down selecting materials for NGNP AHTRs with greater confidence, less effort spent on expensive experimental work, and in shorter periods of time.

# CONTENTS



# FIGURES

## TABLES

# Thermodynamic Assessment of Hot Corrosion Mechanisms of Superalloys Hastelloy N and Haynes 242 in Eutectic Mixture of Molten Salts KF and $ZrF_4$

## 1. INTRODUCTION

The KF-$ZrF_4$ quasi-binary system was considered for application as a heat exchange agent (coolant) in molten salt nuclear reactors (MSRs), beginning with the work carried out at Oak Ridge National Laboratory (ORNL) in the early to mid fifties.[1,2] Based on a combination of such properties as excellent thermal conductivity, low viscosity in the molten state, and other desirable thermo-physical and rheological properties, KF-$ZrF_4$ was selected as a possible candidate for the nuclear reactor secondary heat exchanger loop.

There is currently a renewed interest in using next generation MSRs for such potential applications as molten eutectic mixtures, advanced high temperature reactors (AHTRs), temporary energy storage, and the pyrolysis of hydrocarbons.[3] While most thermo-physical properties of KF-$ZrF_4$ mixtures have been studied in great detail, information on their interactions (generally described as hot corrosion) with the metallic materials used in secondary heat exchanger loops, or any guidance on the down-selection of such materials for minimizing detrimental interactions, is absent for this particular system. A significant body of experimental work on hot corrosion studies was carried out at the University of Wisconsin under the guidance of Professor Paul Allen,[4,5] but his work was done for KF-LiF-NaF molten eutectic mixtures, not for the KF-$ZrF_4$ system.

Even a limited work aimed at the thermodynamic modeling of hot corrosion of such alloys as Haynes 242 and Hastelloy N, represents significant value in terms of predicting the major possible outcomes of corrosion processes, as well as guiding the material down-selection process. It is for this reason that superalloys Haynes 242 and Hastelloy N, widely used for the application as heat exchanger materials, were chosen for thermodynamic modeling of hot corrosion.

The results presented in this report include the following work stages:

1. All available experimental data in the LiF-$ZrF_4$ system, including phase equilibria and thermodynamic properties, were summarized and critically evaluated.
2. An effort was made at the self-consistent assessment of these data in order to come up with a reasonably reliable thermodynamic model of different molten mixtures of KF and $ZrF_4$.
3. Based on the effort of this assessment, it was concluded that the existing data do not allow for a reliable model construction based on both phase equilibria and thermodynamic properties, and a simple “ideal solution” model for the molten salt phase was developed based just on the properties of KF and $ZrF_4$.
4. Thermodynamic models of Haynes 242 and Hastelloy N were constructed and satisfactorily described using the Thermo Tech commercial database TTNi8.
5. Interaction of the eutectic molten mixture of KF and $ZrF_4$ with both alloys was modeled, and the potential mechanisms of hot corrosion were established.
6. Finally, conclusions were made, and the recommendations for the follow-up work were outlined.

# 2. PHASE EQULIBRIA AND THERMODYNAMIC PROPERTIES OF KF-ZRF$_4$ SYSTEM – A LITERATURE REVIEW

In spite of the significance of this pseudo-binary system for the design and successful operation of the next generation nuclear plant MSR reactor, surprisingly little is known about it. The corresponding phase diagram, along with a number of other important systems, were constructed as presented in References 1 and 2 and Figure 1.[1]

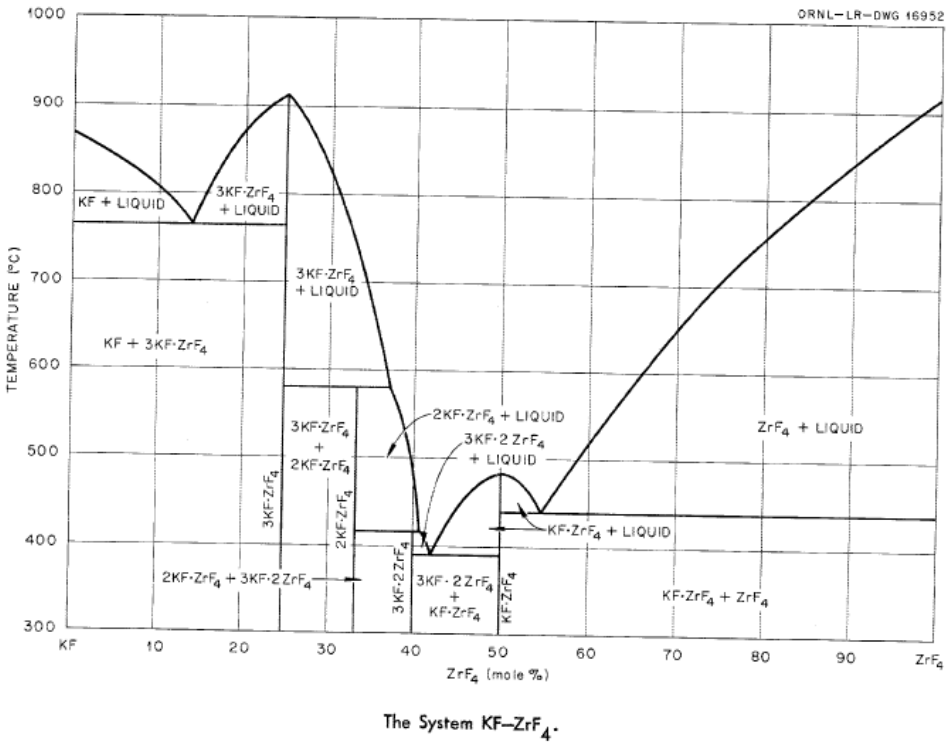


The System KF–ZrF$_4$.

**Figure 1. The KF-ZrF4 pseudo-binary phase diagram, after.[1,2]**

As expected, this phase diagram is qualitatively similar to those for the LiF-ZrF$_4$, NaF-ZrF$_4$, and RbF-ZrF$_4$ phase diagrams.[1] It is characterized by the presence of four intermediate compounds: KF-ZrF$_4$ and 3KF-ZrF$_4$ (melting congruently) and 3KF-2ZrF$_4$ and 2KF-ZrF$_4$ forming according to the peritectic phase reactions (incongruent melting). The temperatures of melting of individual compounds KF and ZrF$_4$ are well established and are correspondingly equal to 858 and 910°C.[6] Their crystalline structures are presented in Figure 2.

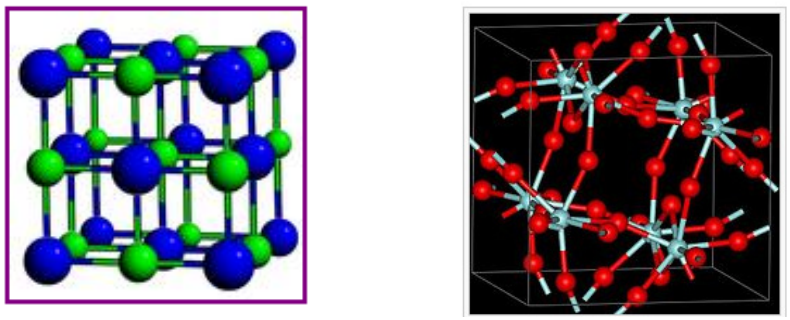

**Figure 2. Crystalline structures of KF (left) and tetrahedral modification of ZrF$_4$.[7]**

KF has the crystalline structure of the B1 type (rock salt; Pearson's symbol cF8; *Strukturbericht* designation B1; space group $Fm\bar{3}m$). Depending on temperature, $ZrF_4$ has three polytypes: α (monoclinic), β (tetragonal, Pearson symbol tP40, space group P42/m), and γ (unknown structure). The unstable β and γ phases irreversibly transform into the α phase at 400°C.[8] In hot corrosion studies of superalloys in molten KF-$ZrF_4$, the crystalline compound that undergoes melting (possibly rendering some of its short-range order structure to ionic liquid) is of the principal interest. Zirconium fluoride is used as a zirconium source in oxygen-sensitive applications such as metal production, similar to the electrolytic reduction of aluminum, magnesium, and titanium).[8]

Thermodynamic data for pure substances KF and $ZrF_4$ are available from the SSUB4 public database. The information in Tables 1 and 2 is available for $ZrF_4$.

**Table 1. Thermodynamic data for pure $ZrF_4$[9], in the SI units**

```
              O U T P U T  F R O M  T H E R M O - C A L C
              2012. 2. 1                              9.29.53

 Phase : F4ZR1_S                    Pressure :      100000.00
 Specie: F4ZR1
*******************************************************************************
    T      Cp            H             S               G
   (K)    (Joule/g K)      (Joule)      (Joule/g K)      (Joule)

*******************************************************************************
  298.15   1.03700E+02  -1.91130E+06   1.04600E+02  -1.94249E+06
  300.00   1.03830E+02  -1.91111E+06   1.05242E+02  -1.94268E+06
  400.00   1.10627E+02  -1.90038E+06   1.36054E+02  -1.95480E+06
  500.00   1.16977E+02  -1.88900E+06   1.61430E+02  -1.96971E+06
  600.00   1.22913E+02  -1.87700E+06   1.83288E+02  -1.98697E+06
  700.00   1.28447E+02  -1.86443E+06   2.02656E+02  -2.00629E+06
  800.00   1.33583E+02  -1.85132E+06   2.20148E+02  -2.02744E+06
  900.00   1.38326E+02  -1.83772E+06   2.36159E+02  -2.05027E+06
 1000.00   1.42674E+02  -1.82367E+06   2.50962E+02  -2.07463E+06
 1100.00   1.46630E+02  -1.80920E+06   2.64749E+02  -2.10043E+06
$ Stable phase is F4ZR1_L
 1200.00   1.50000E+02  -1.73336E+06   3.29228E+02  -2.12843E+06
 1300.00   1.50000E+02  -1.71836E+06   3.41234E+02  -2.16196E+06
 1400.00   1.50000E+02  -1.70336E+06   3.52351E+02  -2.19665E+06
 1500.00   1.50000E+02  -1.68836E+06   3.62699E+02  -2.23241E+06
 1600.00   1.50000E+02  -1.67336E+06   3.72380E+02  -2.26917E+06
 1700.00   1.50000E+02  -1.65836E+06   3.81474E+02  -2.30686E+06
 1800.00   1.50000E+02  -1.64336E+06   3.90048E+02  -2.34544E+06
 1900.00   1.50000E+02  -1.62836E+06   3.98158E+02  -2.38486E+06
 2000.00   1.50000E+02  -1.61336E+06   4.05852E+02  -2.42506E+06

  Phase : F4ZR1_S                    Pressure :      100000.00
  Specie: F4ZR1
```

**Table 2. Thermodynamic data for pure KF [9], in the SI units**

```
              O U T P U T   F R O M   T H E R M O - C A L C
              2012. 2. 1                                9.29. 8
 Phase : F1K1_S                    Pressure :      100000.00
 Specie: F1K1
*******************************************************************************
    T      Cp            H             S               G
   (K)    (Joule/K)      (Joule)      (Joule/K)      (Joule)

*******************************************************************************
  298.15   4.89821E+01  -5.68606E+05   6.65470E+01  -5.88447E+05
  300.00   4.90270E+01  -5.68515E+05   6.68501E+01  -5.88570E+05
  400.00   5.10513E+01  -5.63506E+05   8.12467E+01  -5.96004E+05
  500.00   5.27109E+01  -5.58316E+05   9.28200E+01  -6.04726E+05
  600.00   5.42747E+01  -5.52967E+05   1.02569E+02  -6.14508E+05
  700.00   5.58348E+01  -5.47461E+05   1.11052E+02  -6.25198E+05
  800.00   5.74298E+01  -5.41798E+05   1.18612E+02  -6.36688E+05
  900.00   5.90781E+01  -5.35974E+05   1.25471E+02  -6.48897E+05
 1000.00   6.11700E+01  -5.29967E+05   1.31798E+02  -6.61764E+05
 1100.00   6.38478E+01  -5.23720E+05   1.37749E+02  -6.75244E+05
$ Stable phase is F1K1_L
 1200.00   7.19648E+01  -4.89565E+05   1.67844E+02  -6.90978E+05
 1300.00   7.19648E+01  -4.82368E+05   1.73604E+02  -7.08054E+05
 1400.00   7.19648E+01  -4.75172E+05   1.78938E+02  -7.25685E+05
 1500.00   7.19648E+01  -4.67976E+05   1.83903E+02  -7.43829E+05
 1600.00   7.19648E+01  -4.60779E+05   1.88547E+02  -7.62454E+05
 1700.00   7.19648E+01  -4.53583E+05   1.92910E+02  -7.81529E+05
 1800.00   7.19648E+01  -4.46386E+05   1.97023E+02  -8.01028E+05
 1900.00   7.19648E+01  -4.39190E+05   2.00914E+02  -8.20927E+05
 2000.00   7.19648E+01  -4.31993E+05   2.04606E+02  -8.41204E+05
```

The free energies of the KF and $ZrF_4$ formation are $\Delta_f G°(KF) = -452$ kJ/mol and $\Delta_f G°(ZrF4) = -1552$ kJ/mol respectively.[10] Given the established phase reactions of the formation of intermediate compounds, it is easy to assess the free energies of formation of some intermediate compounds. For example, the case of the phase reaction K2ZrF6 = 2KF + ZrF4 will yield

$\Delta_f G°(K_2ZrF_6) \leq 2(-452)-1552 = -2456$ kJ/mol.

Data on thermodynamic properties of some KF-$ZrF_4$ mixtures and an attempt of modeling phase equilibria in the ternary $BaF_2$-KF-$ZrF_4$ system are published in References 11 and 12. Using high temperature calorimetry, the authors measured the enthalpies of formation of the following molten salt mixtures: LiF+$ZrF_4$ at $T = 1150$ K with $0 < x_{ZrF4} < 0.809$ NaF+$ZrF_4$ at $T = 1282$ K and $0 < x_{ZrF4} < 0.504$ KF+$ZrF_4$ at $T = 1160$ K and $0 < x_{ZrF4} < 0.652$ RbF+$ZrF_4$ at $T = 1090$ K and $0 < x_{ZrF4} < 0.701$.

Special attention was given to limiting $ZrF_4$ losses by evaporation. The uncertainty of the enthalpies is because of mixing ranges from 12% (LiF+$ZrF_4$) to 3% (RbF+$ZrF_4$). The enthalpies of formation of the liquid mixtures were calculated using the value of the enthalpy of fusion proposed by McDonald et al,[13]. For all systems, enthalpies of mixing were found to be strongly exothermal, with minima shifted towards alkali fluoride-rich compositions. From the same measurements it was possible to check some points of equilibrium phase diagrams and to evaluate the enthalpies of formation and of fusion of $3KF \cdot ZrF_4$.

**Table 3. Phase reactions, equilibrium temperatures, and concentrations after Alekseyeva and Poszipaiko.[14]**

| A Diagram Point | Temperature (°C) | $ZrF_4$ concentration (mol%) | Phase(s) | Phase Reaction |
|---|---|---|---|---|
| **A** | 850 | 0 | KF | Melting |
| **B** | 760 | 13 | KF, $K_3ZrF_7$ | Eutectic |
| **C** | 923 | 25 | $K_3ZrF_7$ | Congruent melting |
| **D** | 848 | 31 | $K_3ZrF_7$<br>$K_5Zr_2F_{13}$ | Peritectic |
| **E** | 680 | 34 | $K_5Zr_2F_{13}$<br>$K_3ZrF_7$ | Peritectic |
| **F** | 585 | 36 | $K_3ZrF_7$<br>δ-$K_2ZrF_6$ | Peritectic |
| **G** | 445 | 41 | δ-$K_2ZrF_6$<br>γ-$K_2ZrF_6$ | Peritectic |
| **H** | 430 | 47 | γ-$K_2ZrF_6$<br>γ-$KZrF_5$ | Eutectic |
| **J** | 455 | 50 | γ-$KZrF_5$ | Congruent melting |
| **K** | 440 | 60 | γ-$KZrF_5$<br>α-$ZrF_4$ | Eutectic |
| **L** | 685 | 73 | α-$ZrF_4$<br>β-$ZrF_4$ | Peritectic |
| **M** | 903±5 | 100 | β-$ZrF_4$ | Melting |

As shown in Figure 1, there are five nonvariant phase equilibrium reactions: two of these are eutectic and the remaining three are peritectic reactions. The equilibrium concentrations and temperatures of these reactions, as well as the melting points of compounds KF-$ZrF_4$ and 3KF-$ZrF_4$, were established in Reference 14 and presented in Table 3. The information on the exact position of the equilibrium liquidus temperatures and concentrations (mono-variant equilibria) for the whole diagram is qualitative and represents just a sketch.

The crystalline structure of KF-$ZrF_4$ ($KZrF_5$) was established in References 15 and 16. Single crystals of this compound were obtained from a stoichiometric melt of KF and ZrF4 (823 K; cooling rate: 3°C/h). KZrF5 crystallizes in the triclinic space group ($P\bar{1}$) with coordination number Z = 6. In [15] it was confirmed that $KZrF_5$ is triclinic ($P\bar{1}$) with a = 7.370(1) A; b=8.461(1) A; and c=10.711(1) A. α=75.04(1)°; β=71.57(1)°; and γ=66.13(2)°, with coordination number Z=6. The crystal structure was refined from 5056 reflections. According to Reference 11, this crystal structure is built of corner and edge-sharing $Zr^{IV}F_8$ polyhedra stacked parallel to the (111) plane; these $ZrF_5^{-1}$ layers are held together by potassium cations, $K^+$.[16]

The 3KF-$ZrF_4$, or $K_3ZrF_7$ compound was characterized in Reference 17 and the Landolt-Borstein database by Springer Materials (P. Villars, K. Cenzual, J. Daams, R. Gladyshevskii, O. Shcherban, V. Dubenskyy, N. Melnichenko-Koblyuk, O. Pavlyuk, S. Stoiko, and L. Sysa).[18] Unfortunately, we could not get access to this expensive database.

The structure of molten salt mixtures and crystalline compounds 2KF-$ZrF_4$ (or $K_2ZrF_6$) and 3KF-$ZrF_4$ were studied in Reference 18 using the technique of Raman spectroscopy. Raman spectra of $ZrF_4$–KF molten mixtures have been measured at compositions up to 66 mol% $ZrF_4$ and at temperatures up to 1000°C. The data indicate that in mixtures rich in alkali fluoride, two kinds of chemical species predominate the melt structure: octahedral $ZrF_6^{2-}$ ($\nu_1(A_{1g})$ 570 $cm^{-1}$ and $\nu_5$ ($F_{2g}$) 248 $cm^{-1}$), and pentagonal bipyramidal $ZrF_7^{3-}$ ($\nu_1(A_1')$ 535 $cm^{-1}$ and $\nu_9(E_2')$ 340 $cm^{-1}$). An equilibrium is established between the two species that depends on temperature and composition. Spectral changes upon melting $A_2ZrF_6$ (A = Li or K) and $A_3ZrF_7$ (A = K or Cs) polycrystalline compounds support the proposed two species equilibrium scheme. At 33 mol% $ZrF_4$ the predominant species present are $ZrF_6^{2-}$ octahedra. With increasing $ZrF_4$ mole fraction, the strong $\nu_1(A_{1g})$ band at 570 $cm^{-1}$ shifts continuously to higher wave numbers and new bands appear in the spectra. At the maximum composition of 66 mol% $ZrF_4$, the spectra are characterized by two polarized (630 $cm^{-1}$, strong and ≈ 500 $cm^{-1}$, weak) and two weak depolarized bands are 245 and ≈ 180 $cm^{-1}$. The observed spectral trends with variation of composition were interpreted with a model where the structure of the rich in $ZrF_4$ melts is dominated by small size chains formed by "$ZrF_6$" octahedral.[18]

More specifically, the following schematic was proposed explaining the formation of different complex anions as a function of the $ZrF_4$ molar fraction in the melt[18]:

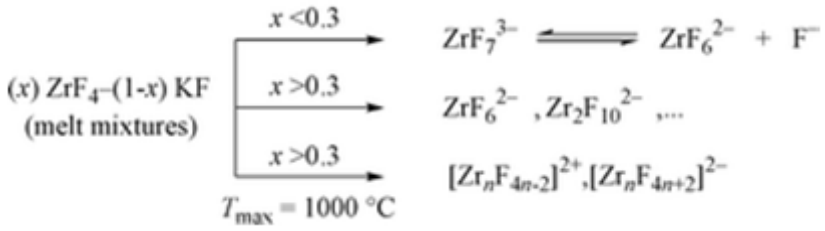


The following potassium zirconates were synthesized in Reference 18: $K_3ZrF_7$ ; $K_2ZrF_6$; δ–$KZrF_5$; γ–$KZrF_5$; and $KZrF_5$. Structural and x-ray luminescence characteristics of zirconium (hafnium) fluoride compounds are presented in Table 4.[18]

**Table 4. Structural and x-ray luminescence characteristics of zirconium (hafnium) fluoride compounds.**

| Compound | Polyhedron* | $CN_{Zr}$ | Types of bridging bonds | Average M–F distances, Å** | Luminescence maximum | |
|---|---|---|---|---|---|---|
| | | | | | λ, nm | intensity, arb. units |
| $K_3ZrF_7$ | $ZrF_7$ | 7 | – | – | None | |
| $Na_5Zr_2F_{13}$ | $ZrF_7$ | 7 | A | 2.35 | – | 0.006 |
| β-$Na_2ZrF_6$ | $ZrF_7$ | 7 | B | 2.49 | 390 | 0.017 |
| $K_2ZrF_6$ | $ZrF_8$ | 8 | B | 2.90 | 320 | 0.510 |
| $Rb_2ZrF_6$ | $ZrF_6$ | 6 | – | 3.04 | 350 | 0.600 |
| $Cs_2ZrF_6$ | $ZrF_6$ | 6 | – | 3.18 | 350 | 0.460 |
| $KZrF_5$ | $ZrF_8$ | 8 | A, B | – | – | – |
| γ-$KZrF_5$ | Data are absent | | | | 330 | 0.275 |
| δ-$KZrF_5$ | Data are absent | | | | 360 | 0.065 |
| $K_2HfF_6$ | $HfF_8$ | 8 | B | 2.85 | 310 | 0.330 |

The types of bridging bonds A and B correspond to the following structures; $CN_{Zr}$ represents the coordination number of Zr atoms in a given structure:[18]

A, Zr–F–Zr; B, 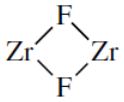


## 3. CONSTRUCTION OF A SIMPLIFIED THERMODYNAMIC MODEL FOR THE KF-ZRF$_4$ MOLTEN SALTS

In general, self-consistent assessment of thermodynamic data and phase equilibria represents a complex problem requiring execution of several tasks outlined in Figure 3.

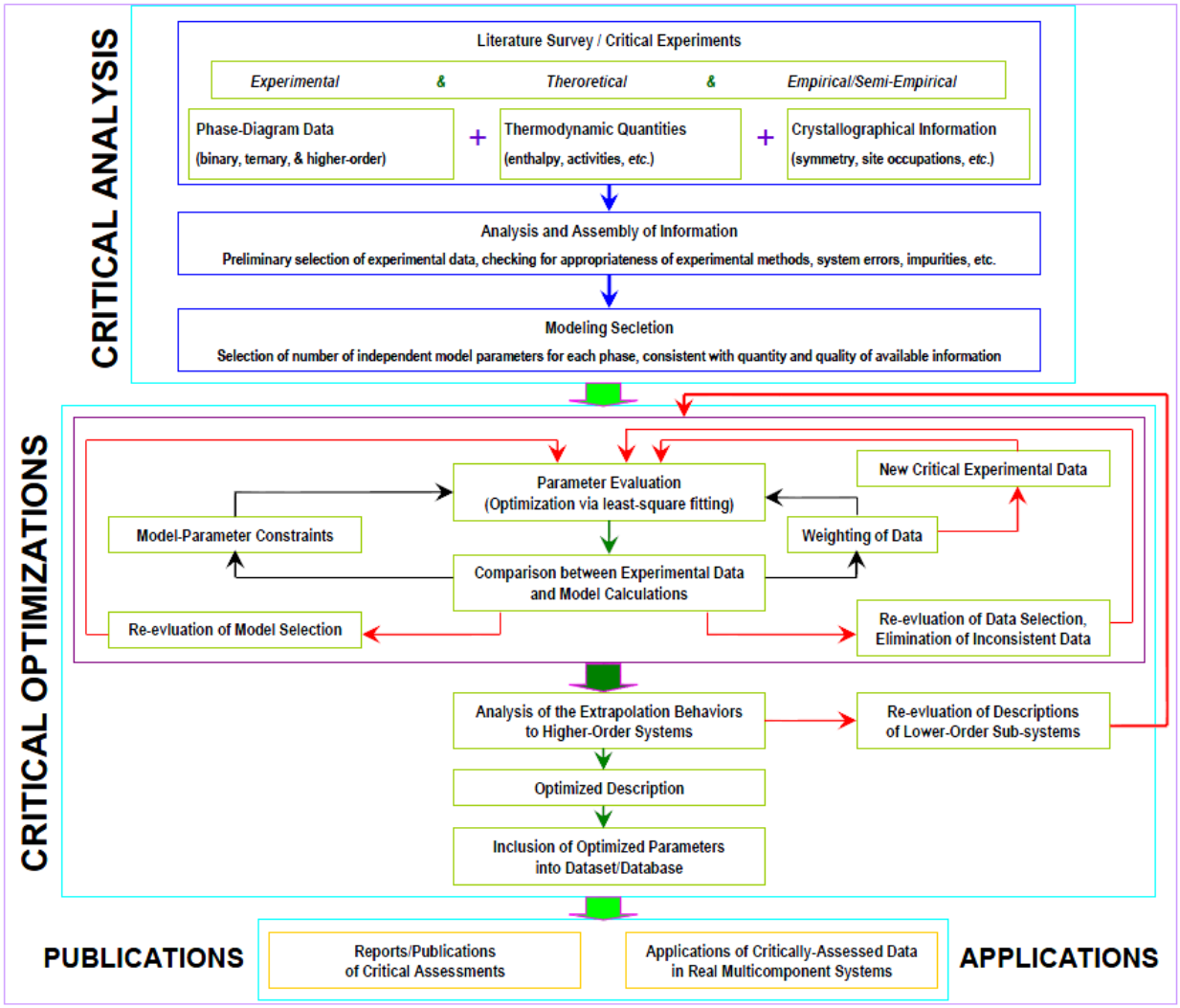


**Figure 3. CALPHAD ("CALculation of PHAse Diagrams") approach to assessment of thermodynamic and phase diagram data.[9]**

As it follows from Figure 3, the key requirement to successful optimization and assessment is sufficient amount of data on thermodynamic properties of components, intermediate phases, solid solutions, and the liquid phase.

From the literature review conducted in Section 2 above, it becomes quite obvious that the construction of a rigorous thermodynamic model of the KF-$ZrF_4$ molten salt mixtures is practically impossible. Indeed, the experimental phase equilibria data found, relates only to the temperatures of melting of the both compounds and to the temperatures and compositions corresponding to the six invariant phase reactions in this system. Any experimental data on phase equilibria in the solid state is practically absent; in the liquid phase, any data on the liquidus temperatures is completely absent.

Available thermodynamic data is also scarce. Free energies of formation, heat capacities, and their thermal dependencies for the KF and $ZrF_4$ terminal compounds (the public domain thermodynamic database for pure substances SSUB4 was used for that purpose) were established. The free energies of formation of a number of intermediate compounds in this system were also calculated, using simple rules of thermochemistry. However, these are not experimental values, and any information on the temperature dependence of heat capacity in the solid state is absent. There is just one experimental point for heat capacity in the liquid phase—at the composition corresponding to the deep eutectic in this system, $c_p$= 1051 J/kg K,[1] which is assumed to be independent of temperature.

One could use the sketch phase diagram given in References 1 and 2 for this situation, then use an appropriate digitizing software (www.digitizeit.de is a good product) and convert at least some portions of the liquidus curve into experimental data. Then, using these experimental points and calculated values of the free energies for all compounds, try to use the optimization module called PARROT (a part of the Thermo-Calc software[9]) to try and achieve a reasonable agreement between experiment and calculations. However, even assuming the simplest possible variant (complete absence of solubility on the basis of all individual compounds, their ideal behavior in the solid phase, and an ideal solution model in the liquid phase described in the thermo-chemical module of the Thermo-Calc called GIBBS) and a very robust Levenberg-Marquardt optimization routine[9] used in Thermo-Calc, we would inevitably end up trying to solve inverse ill-posed problems of experimental data reconstruction. In this case, one would be trying to use the experimental phase diagram to obtain information on the thermodynamic properties of the mixtures. A similar situation was encountered when working on inverse ill-posed problems of computational thermodynamics in 1987, trying to reconstruct excess thermodynamic functions of binary Cr-Si and V-Si alloys using just data on the corresponding phase equilibria.[19] On that basis, it was quite straightforward to calculate all excess thermodynamic functions of materials using the same model assumptions. However, even perturbing experimental phase equilibria data within the limits of experimental error can change thermodynamic functions dramatically. In many cases, there is a significant discrepancy between the enthalpy of mixing values in these two calculations, but the excess entropy of mixing could actually change its sign.[19]

Such ill-posed problems, from a mathematical perspective, were described for the first time by a French mathematician Adamard.[20] The three conditions defining a well-posed problem are that its solution must exist, be unique, and be stable with respect to small perturbations in the input data. In this case, the lack of solution uniqueness manifests itself in computations in a very significant sensitivity of the results with respect to minor changes in experimental information on phase equilibria. A mathematical trick used in Reference 19 to overcome the inherent instability of the problem: using the Tikhonov regularization technique and minimizing a modified quadratic functional ensured that the average experimental error was equal to the error in experiments, instead of minimizing the latter as in conventional global optimization techniques.[21]

Another excellent example pointing in the same direction was given by Lukas, Fries, and Sundman,[22] who considered a hypothetical situation of assessing a binary system A-B in the absence of any thermodynamic data. They demonstrated that using the thermodynamic models with and without ordering in the solid phase, the phase diagrams were remarkably similar; but a very significant difference was observed in the predicted thermodynamic properties of materials[22] (also see References 23 and 24).

But, in the present case, with the exception of pure KF and ZrF4, even experimental data on phase equilibria in the KF-$ZrF_4$ system is missing, not to mention any thermodynamic results. This situation makes any self-consistent assessment effort hopeless.

This situation therefore calls for a different, albeit simplified approach that at least provided some guidance in terms of the possible outcomes of hot corrosion of Hastelloy N and Haynes 242, as was done for this report.

Using the public domain database for pure substances, SSUB4, thermo-chemical data for both KF and $ZrF_4$ (see Table 1 and Table 2) were extracted. In order to construct a thermodynamic model of the liquid phase, the approximation of ideal solutions was used, without any adjustable parameters. Finally, a liquid solution was obtained corresponding to the eutectic point as determined from the corresponding simple eutectic phase diagram constructed on the basis of this model. All subsequent extractions were carried with this model of the liquid phase.

The constructed database is described in Appendix A, Thermo-Calc script in Appendix B, and the corresponding phase diagram is given in Figure 4 below:

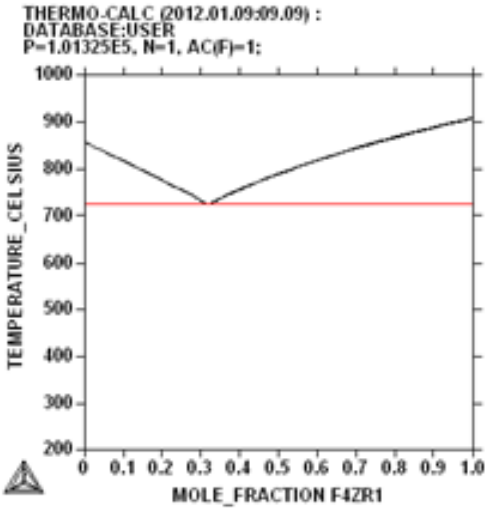


**Figure 4. Phase diagram KF-$ZrF_4$ constructed under the assumption of the ideal behavior of liquid phase.**

The results of work of the Thermo-Calc script (computation of $ZrF_4$-KF phase diagram) are presented in Appendix C.

It is very important to understand the limitations of the adopted approach. In turn, to achieve this goal, one needs to have a clear idea of the assumptions that were made in this process. These assumptions are as follows:

- A full assessment of the phase diagram was not performed with all four of its intermediate compounds
- It was assumed that there is no solubility of solid KF in all three of the polytypes of $ZrF_4$ in solid KF, and that there is no solubility of solid polytypes of $ZrF_4$ in solid KF
- It was assumed that any mixture of molten salts KF and $ZrF_4$ can be described using the ideal solution model.

This corresponds, in fact, to assuming that a simple eutectic diagram (without any intermediate compounds) would be satisfactory to predict the behavior of a eutectic molten salt composition and to use it in all subsequent work on hot corrosion of superalloys.

How reasonable are these assumptions? As far as mutual solubility of KF and $ZrF_4$ is concerned, one can be quite confident that neglecting it is reasonable because of the different crystalline structure of KF and $ZrF_4$ (rock salt cubic for KF versus tetragonal or monoclinic for $ZrF_4$). Using the well-established Richardson extrapolation procedure also does not raise any serious suspicions because the thermodynamic data for the pure substances (and the errors of their measurement) are very well established. Perhaps the most serious reason for concern is omitting all of the four intermediate compounds from calculations. Indeed, one would probably need to use some variant of the sublattice model[23] with ordering to adequately describe these complex phases in the solid state. Furthermore, the existing Raman spectroscopy data leave no doubt about short-range ordering in the liquid phase and the existence of complex anions (e.g., $ZrF_6^{2-}$ and $Zr_2F_{10}^{2-}$ coordinated with cations of $K^+$).[17] In our calculations, we had to neglect these effects. Still, the behavior of strongly associated molten salt mixtures with significant negative deviations from ideality is much better represented by the ionic liquid model.[25] Nevertheless, in the absence of more detailed information on thermodynamic properties and phase equilibria, there is no choice but to adopt this simplified approach, which is justified because experimental work with molten salts is very costly and requires special equipment and training. Some of the hot corrosion work is planned to proceed at the University of Wisconsin later in 2012. This work will compare the results of predictions made in this report to valuable experimental information.

One fundamental approach completely omitted in this research effort is the application of the first-principles atomistic algorithms for obtaining information about thermodynamic properties of intermediate compounds.[26,27] Crystalline lattices for $K_2ZrF_6$ and $KZrF_5$ are well-known along with the Wykoff positions of all atoms in the lattice. It is certainly worth exploring whether such codes as VASP[28] could be helpful in generating such information. The research group does not have license for and access to VASP at this time. This work will commence later on in 2012/2013.

# 4. THERMODYNAMIC MODELS OF HAYNES 242 AND HASTELLOY N ALLOYS

## 4.1 Haynes 242

Haynes 242 was developed more than 40 years ago, so its properties, microstructure, and behavior in oxidizing environments have been extensively studied.[29] Typically, quasi-binary diagrams (property diagrams) are constructed and used to help better understand a metal's phase composition as a function of temperature and pressure.[22,23] Today, such diagrams can be studied using well-regressed thermodynamic databases and fast, efficient algorithms of the global Gibbs energy minimization to establish equilibrium conditions.

In order to probe the microstructure of Haynes 242 at temperatures from 600 to 720°C, the carbon isopleth was constructed. As shown in Figure 5, Haynes 242 is an austenitic matrix alloy with particles of $Ni_2(Cr,Mo)$ and, depending upon its heat treatment, μ-phase, δ–phase, and γ'-precipitates.

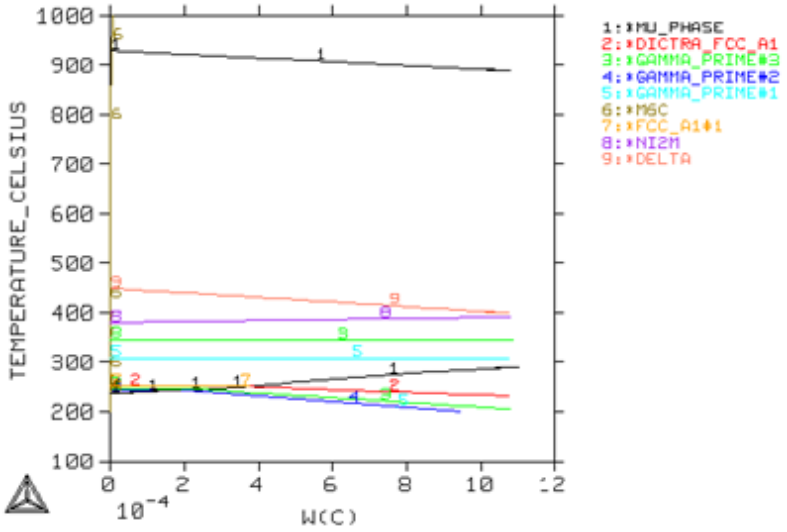


**Figure 5. Carbon isopleth for Haynes 242.**

A microstructural characterization of a Haynes 242 nickel-molybdenum-chromium superalloy was performed.[29] Molybdenum was found mostly in the $Ni_2(Mo,Cr)$ precipitates, whereas iron, aluminum, silicon, manganese, and nickel entered mostly the austenitic FCC-matrix. Chromium was not found to partition significantly between the phases. Atom probe tomography and energy-filtered transmission electron microscopy revealed boron, molybdenum, chromium, phosphorus, and carbon segregation to the grain boundaries. In spite of the size of the precipitates being larger after a two-step heat treatment of 16 hours at 704°C + 16 hours at 650°C compared to a one-step heat treatment of 48 hours at 650°C, no significant differences were found in the mechanical properties or compositions of the phases.[29]

The formation of the $Ni_2M$ intermetallic phase takes place at temperatures around 400°C as shown in Figure 5. However, overall, this is a reasonable set of phases to be expected for Haynes 242 at this temperature range because the alloy's ultimate microstructure and phase composition will be determined by the heat treatments used during thermomechanical processing.

## 4.2 HASTELLOY *N*

Hastelloy N is a nickel-base alloy invented at ORNL as a container material for molten fluoride salts. The hot corrosion mechanism of Hastelloy N has been studied extensively as reported by McKoy, Jr.[30] It has good oxidation resistance to hot fluoride salts in the temperature range of 704 to 871°C.

The carbon isopleth (property diagram) of this alloy was constructed similar to Figure 6. The equilibrium phases for Hastelloy N represented in this Figure are carbide $M_6C$, γ' phase (strengthening precipitates), and μ–phase,[28] similar to Haynes 242, but no $Ni_2M$ formation is expected in this case.

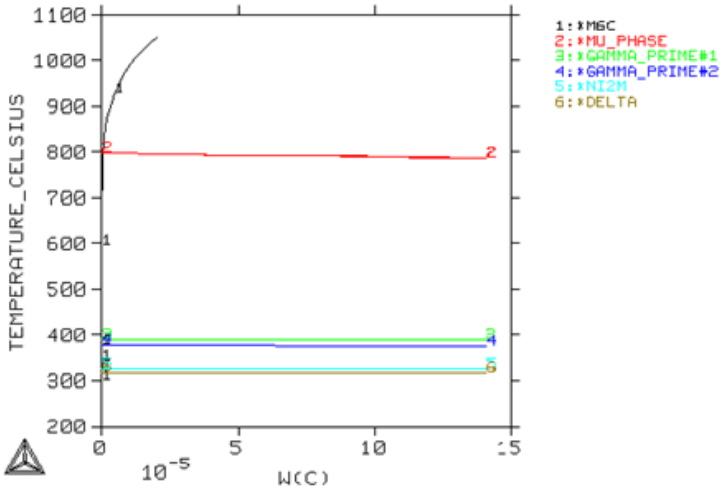


**Figure 6. Carbon isopleths for *Hastelloy N* superalloy with generic composition.**

# 5. MODELING OF HOT CORROSION OF ALLOYS HAYNES 242 AND HASTELLOY N IN EUTECTIC MIXTURE OF MOLTEN SALTS KF-$ZRF_4$

The quantitative assessment of hot corrosion for such complex multicomponent alloys as Haynes 242 or Hastelloy N is extremely complicated from the computational thermodynamics perspective. The need to work with at least three data bases (TTNI8; our own USER database - KFZRF4; and SSUB4 (for superalloys, molten salts, and pure substances) rapidly makes the overall number of competing phases astronomical. In such a situation, even a high-quality global equilibrium solver may yield unphysical results. To make this problem more tractable, the researcher needs to reduce the number of components in the system without jeopardizing the quality of the results, making reasonable assumptions about phases that might be formed at conditions of interest and a realistic representation of the initial set of phases in the system.

After tedious computer experimentation, it was decided to reduce Haynes 242 and Hastelloy N to simplified alloys with similar compositions. More specifically, it was assumed that the behavior of multicomponent alloy Haynes 242 can be realistically described using just four components: molybdenum, iron, chromium, and nickel. In such a formulation, the composition of alloy Hastelloy N in weight-percent (wt%) is given as: Ch-7.2%, Mo-16.8%, and Fe- ~0.5%, with the balance being nickel. Proceeding in a similar fashion, Haynes 242 gives: Ch-8.1%, Mo-24.7%, and Fe-1.4%, with the balance being nickel (65.2%).

Since the quasi-binary system KF-$ZrF_4$ was not assessed in a database for the ionic liquids (SALT1), the simplified modeling described above was used. A Thermo-Calc script was prepared to the model hot corrosion process at ~740°C. This script, given in Appendix D, shows that all calculations were made for 1 mole of the "Alloy 242 + molten salt" mixture at ambient pressure. Since the working temperature of the AHTR secondary loop coolant was supposed to be 700°C, this assumption seems to be reasonable. The script for this work is presented in Appendix E.

The results presented in Figure 7 were obtained from a so-called single-point equilibrium calculation. These results provide a very reasonable equilibrium picture for both alloys—FCC-matrix, and a small amount of the μ-phase. There is also a molten-salt phase and a very small amount of solid $CrF_2$ (denoted with the grey oval in Figure 7). This latter result is very important because it demonstrates how the process of corrosion of Haynes 242 could begin by leaching chromium from the alloy's composition.

The results for hot corrosion of Alloy 242 at lower concentrations of fluorine, $x(F) = 10^{-12}$ and $x(F) = 10^{-13}$, are presented in Figures 8 and 9. Small concentrations of elemental fluorine above molten fluoride mixtures are always present due to dissociation of the salts into ionic liquids and evaporation.

The next step was to assess how the hot corrosion process might develop if the concentration of fluorine varied in the case of Hastelloy N, so that the severity of a hot corrosion attack could be compared for Haynes 242 and Hastelloy N.

Proceeding in a way similar to the case of Haynes 242, the following results presented in Figures 10, 11, and 12 were obtained. The most important finding was that Hastelloy N is less prone to hot corrosion than Haynes 242.

```
N=1, P=1E5, T=1013, X(NI)=0.326, X(CR)=4E-2, X(MO)=0.124, X(FE)=1E-2,
   X(F1K1)=0.34, X(F)=1E-11
DEGREES OF FREEDOM 0

Temperature   1013.00 K (   739.85 C),  Pressure  1.000000E+05
Number of moles of components  1.00000E+00,  Mass in grams  8.01744E+01
Total Gibbs energy -5.83121E+05,  Enthalpy -4.41424E+05,  Volume
).00000E+00

Component               Moles       W-Fraction  Activity  Potential Ref.stat
F1K1                    3.4000E-01  2.4637E-01 5.8566E-35 -6.6389E+05 SER
F4ZR1                   1.6000E-01  3.3370E-01 6.516E-108 -2.0787E+06 SER
F                       7.7504E-12  1.8365E-12 1.4059E-22 -4.2379E+05 SER
NI                      3.2600E-01  2.3864E-01 2.8976E-03 -4.9220E+04 SER
CR                      4.0000E-02  2.5941E-02 6.9047E-04 -6.1301E+04 SER
MO                      1.2400E-01  1.4838E-01 4.9078E-03 -4.4782E+04 SER
FE                      1.0000E-02  6.9657E-03 1.3858E-04 -7.4827E+04 SER

LIQUID_SALT                 Status ENTERED     Driving force  0.0000E+00
Moles 5.0000E-01, Mass 4.6507E+01, Volume fraction 0.0000E+00 Massfractions:
F4ZR1  5.75272E-01  MO     0.00000E+00  NI     0.00000E+00  FE 0.00000E+00
F1K1   4.24728E-01  CR     0.00000E+00  F      0.00000E+00

FCC_A1                      Status ENTERED     Driving force  0.0000E+00
Moles 3.1427E-01, Mass 1.9800E+01, Volume fraction 0.0000E+00 Massfractions:
NI     7.21157E-01  CR     5.91766E-02  F4ZR1  2.65405E-12  F-1.20617E-12
MO     1.98678E-01  FE     2.09888E-02  F1K1   0.00000E+00

MU_PHASE                    Status ENTERED     Driving force  0.0000E+00
Moles 1.8573E-01, Mass 1.3868E+01, Volume fraction 0.0000E+00 Massfractions:
MO     5.74182E-01  CR     6.54856E-02  F1K1   0.00000E+00 F4ZR1 0.00000E+00
NI     3.50029E-01  FE     1.03041E-02  F      0.00000E+00

CR1F2_S                     Status ENTERED     Driving force  0.0000E+00
Moles 1.3511E-11, Mass 4.0530E-10, Volume fraction 0.0000E+00 Massfractions:
CR     5.77785E-01  F1K1   0.00000E+00  NI     0.00000E+00 F4ZR1 0.00000E+00
```

**Figure 7. Hot corrosion of Haynes Alloy 242 at fluorine concentration x(F)=$10^{-11}$.**

```
N=1, P=1E5, T=1013, X(NI)=0.326, X(CR)=4E-2, X(MO)=0.124, X(FE)=1E-2,
    X(F1K1)=0.34, X(F)=1E-12  DEGREES OF FREEDOM 0

 Temperature   1013.00 K (   739.85 C),  Pressure  1.000000E+05
 Number of moles of components  1.00000E+00,  Mass in grams  8.01744E+01
 Total Gibbs energy -5.83121E+05,  Enthalpy -4.41424E+05,  Volume 0.00000E+00

 Component               Moles       W-Fraction  Activity  Potential Ref.stat
 F1K1                    3.4000E-01  2.4637E-01 5.8566E-35 -6.6389E+05 SER
 F4ZR1                   1.6000E-01  3.3370E-01 6.516E-108 -2.0787E+06 SER
 F                      -1.2496E-12 -2.9610E-13 1.4059E-22 -4.2379E+05 SER
 NI                      3.2600E-01  2.3864E-01 2.8976E-03 -4.9220E+04 SER
 CR                      4.0000E-02  2.5941E-02 6.9047E-04 -6.1301E+04 SER
 MO                      1.2400E-01  1.4838E-01 4.9078E-03 -4.4782E+04 SER
 FE                      1.0000E-02  6.9657E-03 1.3858E-04 -7.4827E+04 SER

 LIQUID_SALT                 Status ENTERED     Driving force  0.0000E+00
 Moles 5.0000E-01, Mass 4.6507E+01, Volume fraction 0.0000E+00 Massfractions:
 F4ZR1  5.75272E-01  MO     0.00000E+00  NI     0.00000E+00  FE 0.00000E+00
 F1K1   4.24728E-01  CR     0.00000E+00  F      0.00000E+00

 FCC_A1                      Status ENTERED     Driving force  0.0000E+00
 Moles 3.1427E-01, Mass 1.9800E+01, Volume fraction 0.0000E+00 Massfractions:
 NI     7.21157E-01  CR     5.91766E-02  F4ZR1  2.65405E-12  F-1.20617E-12
 MO     1.98678E-01  FE     2.09888E-02  F1K1   0.00000E+00

 MU_PHASE                    Status ENTERED     Driving force  0.0000E+00
 Moles 1.8573E-01, Mass 1.3868E+01, Volume fraction 0.0000E+00 Massfractions:
 MO     5.74182E-01  CR     6.54856E-02  F1K1   0.00000E+00 F4ZR1 0.00000E+00
 NI     3.50029E-01  FE     1.03041E-02  F      0.00000E+00

 CR1F2_S                     Status ENTERED     Driving force  0.0000E+00
 Moles 1.3511E-14,  Mass 3.3741E-13,Volume fraction 0.0000E+00 Massfractions:
 CR     5.77785E-01  F1K1   0.00000E+00  NI     0.00000E+00 F4ZR1 0.00000E+00
 F      4.22215E-01  MO     0.00000E+00  FE     0.00000E+00
```

**Figure 8. Leaching of Cr from alloy Haynes 242 at concentration of fluorine x(F)=$10^{-12}$.**

```
 Conditions:
  N=1, P=1E5, T=1013, X(NI)=0.326, X(CR)=4E-2, X(MO)=0.124, X(FE)=1E-2,
     X(F1K1)=0.34, X(F)=1E-13 DEGREES OF FREEDOM 0
  Temperature   1013.00 K (   739.85 C),  Pressure  1.000000E+05
  Number of moles of components  1.00000E+00,  Mass in grams  8.01744E+01
  Total Gibbs energy -5.83121E+05,  Enthalpy -4.41424E+05,  Volume
 0.00000E+00

  Component               Moles       W-Fraction  Activity  Potential Ref.stat
  F1K1                    3.4000E-01  2.4637E-01 5.8566E-35 -6.6389E+05 SER
  F4ZR1                   1.6000E-01  3.3370E-01 6.516E-108 -2.0787E+06 SER
  F                      -1.2571E-12 -2.9787E-13 1.1773E-22 -4.2529E+05 SER
  NI                      3.2600E-01  2.3864E-01 2.8976E-03 -4.9220E+04 SER
  CR                      4.0000E-02  2.5941E-02 6.9047E-04 -6.1301E+04 SER
  MO                      1.2400E-01  1.4838E-01 4.9078E-03 -4.4782E+04 SER
  FE                      1.0000E-02  6.9657E-03 1.3858E-04 -7.4827E+04 SER

  LIQUID_SALT                 Status ENTERED     Driving force  0.0000E+00
  Moles 5.0000E-01, Mass 4.6507E+01, Volume fraction 0.0000E+00 Massfractions:
  F4ZR1  5.75272E-01  MO     0.00000E+00  NI     0.00000E+00  FE0.00000E+00
  F1K1   4.24728E-01  CR     0.00000E+00  F      0.00000E+00

  FCC_A1                      Status ENTERED     Driving force  0.0000E+00
  Moles 3.1427E-01, Mass 1.9800E+01, Volume fraction 0.0000E+00 Massfractions:
  NI     7.21157E-01  CR     5.91766E-02  F4ZR1  2.65405E-12  F-1.20617E-12
  MO     1.98678E-01  FE     2.09888E-02  F1K1   0.00000E+00

  MU_PHASE                    Status ENTERED     Driving force  0.0000E+00
  Moles 1.8573E-01, Mass 1.3868E+01, Volume fraction 0.0000E+00 Massfractions:
  MO     5.74182E-01  CR     6.54856E-02  F1K1   0.00000E+00 F4ZR1 0.00000E+00
  NI     3.50029E-01  FE     1.03041E-02  F      0.00000E+00
  MO     5.76486E-01  CR     6.15645E-02  F1K1   0.00000E+00 F4ZR1 0.00000E+00
  NI     3.39516E-01  FE     2.24332E-02  F      0.00000E+00
```

**Figure 9. No hot corrosion in alloy Haynes 242 at x(F)=$10^{-13}$.**

```
N=1, P=1E5, T=1013, X(NI)=0.355, X(CR)=3.6E-2, X(MO)=8.4E-2,
X(FE)=2.5E-2, X(F1K1)=0.34, X(F)=1E-11  DEGREES OF FREEDOM 0

 Temperature   1013.00 K (   739.85 C),  Pressure  1.000000E+05
 Number of moles of components  1.00000E+00,  Mass in grams  7.86685E+01
 Total Gibbs energy -5.83585E+05,  Enthalpy -4.41174E+05,  Volume 0.00000E+00

 Component               Moles       W-Fraction  Activity  Potential Ref.stat
 F1K1                    3.4000E-01  2.5109E-01 5.8566E-35 -6.6389E+05 SER
 F4ZR1                   1.6000E-01  3.4008E-01 6.516E-108 -2.0787E+06 SER
 F                       6.9221E-12  1.6716E-12 1.4151E-22 -4.2374E+05 SER
 NI                      3.5500E-01  2.6484E-01 2.8025E-03 -4.9502E+04 SER
 CR                      3.6000E-02  2.3794E-02 6.8151E-04 -6.1411E+04 SER
 MO                      8.4000E-02  1.0244E-01 4.9171E-03 -4.4766E+04 SER
 FE                      2.5000E-02  1.7748E-02 2.8521E-04 -6.8748E+04 SER

 LIQUID_SALT                 Status ENTERED     Driving force  0.0000E +00
 Moles 5.0000E-01, Mass 4.6507E+01, Volume fraction 0.0000E+00 Massfractions:
 F4ZR1  5.75272E-01  MO     0.00000E+00  NI     0.00000E+00  FE 0.00000E+00
 F1K1   4.24728E-01  CR     0.00000E+00  F      0.00000E+00

 FCC_A1                      Status ENTERED     Driving force  0.0000E+00
 Moles 4.2158E-01, Mass 2.6301E+01, Volume fraction 0.0000E+00 Massfractions:
 NI     7.16516E-01  CR     5.74514E-02  F4ZR1  2.68027E-12  F-1.21809E-12
 MO     1.77947E-01  FE     4.80855E-02  F1K1   0.00000E+00

 MU_PHASE                    Status ENTERED     Driving force  0.0000E+00
 Moles 7.8417E-02, Mass 5.8610E+00, Volume fraction 0.0000E+00 Massfractions:
 MO     5.76486E-01  CR     6.15645E-02  F1K1   0.00000E+00 F4ZR1 0.00000E+00
 NI     3.39516E-01  FE     2.24332E-02  F      0.00000E+00

CR1F2_S                      Status ENTERED     Driving force  0.0000E+00
Moles 1.3511E-11, Mass 4.0530E-10, Volume fraction 0.0000E+00 Massfractions:
CR     5.77785E-01  F1K1   0.00000E+00  NI     0.00000E+00 F4ZR1 0.00000E+00
F      4.22215E-01  MO     0.00000E+00  FE     0.00000E+00
```

**Figure 10. Leaching of Cr from alloy Hastelloy N at x(F)=$10^{-11}$.**

```
N=1, P=1E5, T=1013, X(NI)=0.355, X(CR)=3.6E-2, X(MO)=8.4E-2,
X(FE)=2.5E-2, X(F1K1)=0.34, X(F)=1E-12  DEGREES OF FREEDOM 0

 Temperature   1013.00 K (   739.85 C),  Pressure  1.000000E+05
 Number of moles of components  1.00000E+00,  Mass in grams  7.86685E+01
 Total Gibbs energy -5.83585E+05,  Enthalpy -4.41174E+05,  Volume 0.00000E+00

 Component               Moles       W-Fraction  Activity  Potential Ref.stat
 F1K1                    3.4000E-01  2.5109E-01 5.8566E-35 -6.6389E+05 SER
 F4ZR1                   1.6000E-01  3.4008E-01 6.516E-108 -2.0787E+06 SER
 F                      -1.6863E-12 -4.0724E-13 1.3353E-22 -4.2423E+05 SER
 NI                      3.5500E-01  2.6484E-01 2.8025E-03 -4.9502E+04 SER
 CR                      3.6000E-02  2.3794E-02 6.8151E-04 -6.1411E+04 SER
 MO                      8.4000E-02  1.0244E-01 4.9171E-03 -4.4766E+04 SER
 FE                      2.5000E-02  1.7748E-02 2.8521E-04 -6.8748E+04 SER

 LIQUID_SALT                 Status ENTERED     Driving force  0.0000E+00
 Moles 5.0000E-01, Mass 4.6507E+01, Volume fraction 0.0000E+00 Massfractions:
 F4ZR1  5.75272E-01  MO     0.00000E+00  NI     0.00000E+00  FE 0.00000E+00
 F1K1   4.24728E-01  CR     0.00000E+00  F      0.00000E+00

 FCC_A1                      Status ENTERED     Driving force  0.0000E+00
 Moles 4.2158E-01, Mass 2.6301E+01, Volume fraction 0.0000E+00 Massfractions:
 NI     7.16516E-01  CR     5.74514E-02  F4ZR1  2.68027E-12  F-1.21809E-12
 MO     1.77947E-01  FE     4.80855E-02  F1K1   0.00000E+00

 MU_PHASE                    Status ENTERED     Driving force  0.0000E+00
 Moles 7.8417E-02, Mass 5.8610E+00, Volume fraction 0.0000E+00 Massfractions:
 MO     5.76486E-01  CR     6.15645E-02  F1K1   0.00000E+00 F4ZR1 0.00000E+00
 NI     3.39516E-01  FE     2.24332E-02  F      0.00000E+00
```

**Figure 11. Hastelloy N at x(F)=$10^{-12}$ : unlike Haynes 242, no corrosion is observed!**

```
Conditions:
 N=1, P=1E5, T=1013, X(NI)=0.355, X(CR)=3.6E-2, X(MO)=8.4E-2,
X(FE)=2.5E-2,
    X(F1K1)=0.34, X(F)=1E-12
 DEGREES OF FREEDOM 0

 Temperature   1013.00 K (   739.85 C),  Pressure  1.000000E+05
 Number of moles of components  1.00000E+00,  Mass in grams  7.86685E+01
 Total Gibbs energy -5.83585E+05,  Enthalpy -4.41174E+05,  Volume
0.00000E+00

 Component               Moles       W-Fraction  Activity  Potential Ref.stat
 F1K1                    3.4000E-01  2.5109E-01 5.8566E-35 -6.6389E+05 SER
 F4ZR1                   1.6000E-01  3.4008E-01 6.516E-108 -2.0787E+06 SER
 F                      -1.6863E-12 -4.0724E-13 1.3353E-22 -4.2423E+05 SER
 NI                      3.5500E-01  2.6484E-01 2.8025E-03 -4.9502E+04 SER
 CR                      3.6000E-02  2.3794E-02 6.8151E-04 -6.1411E+04 SER
 MO                      8.4000E-02  1.0244E-01 4.9171E-03 -4.4766E+04 SER
 FE                      2.5000E-02  1.7748E-02 2.8521E-04 -6.8748E+04 SER

 LIQUID_SALT                 Status ENTERED     Driving force  0.0000E+00
 Moles 5.0000E-01, Mass 4.6507E+01, Volume fraction 0.0000E+00 Massfractions:
 F4ZR1  5.75272E-01  MO     0.00000E+00  NI     0.00000E+00  FE 0.00000E+00
 F1K1   4.24728E-01  CR     0.00000E+00  F      0.00000E+00

 FCC_A1                      Status ENTERED     Driving force  0.0000E+00
 Moles 4.2158E-01, Mass 2.6301E+01, Volume fraction 0.0000E+00 Massfractions:
 NI     7.16516E-01  CR     5.74514E-02  F4ZR1  2.68027E-12  F-1.21809E-12
 MO     1.77947E-01  FE     4.80855E-02  F1K1   0.00000E+00

 MU_PHASE                    Status ENTERED     Driving force  0.0000E+00
 Moles 7.8417E-02, Mass 5.8610E+00, Volume fraction 0.0000E+00 Massfractions:
 MO     5.76486E-01  CR     6.15645E-02  F1K1   0.00000E+00 F4ZR1 0.00000E+00
 NI     3.39516E-01  FE     2.24332E-02  F      0.00000E+00
```

**Figure 12. Hastelloy N at x(F)=$10^{-13}$: no hot corrosion at these conditions.**

Based on the results obtained for these two alloys under identical conditions, Hastelloy N is less prone to hot corrosion (leaching of $CrF_2$ ) than Haynes 242 because corrosion attack begins for 242 at milder oxidizing conditions.

How significant are these conclusions, and what was omitted during the simulation process? First, it was checked that the results are stable with respect to minor truncation error: similar data were obtained on a Linux machine with a 64-bit machine word, and on a Windows-XP workstation with 32-bit machine word. Secondly, the results obtained in this report are qualitatively similar to the author's previous work where a similar technique was used to compare the stability of these two superalloys with respect to hot corrosion in a eutectic mixture of LF-KF-NaF. In the case of this ternary mixture, the SALT1 database was used that correctly assesses phase equilibria in the corresponding binary systems. The data published earlier by Chartrand and Pelton[31] were used to assess the ternary system.

Because experimental data on the phase equilibria and thermodynamic properties of KF-$ZrF_4$ system was lacking, a significant oversimplification was made by assuming the ideal behavior of salt mixtures in the liquid phase and ignoring the well-proved existence of the four intermediate phases. These assumptions might possibly result in the omission of some potential corrosion mechanisms. For example, after corrosion experiments in an study by Danielik, Fellner, and Matal[32] on the mechanisms of corrosion of pure nickel in a mixture of molten salts Na, LiF, and $ZrF_4$, a layer of solidified LiF, NaF, and mixed salts $Na_3ZrF_7$, $Li_3ZrF_7$, and $Li_2ZrF_6$ was observed, which was beneficial for suppressing further corrosion. A similar phenomenon might take place for the KF-$ZrF_4$ mixture. This modeling study could not take such reactions into account because all of the intermediate phases were ignored during modeling. Other products of corrosion found in Reference [32] were $NiF_2$ and $Zr_2Ni$. A more rigorous thermodynamic model and phase diagram data will need to be taken into account for a better and more accurate assessment.

# 6. CONCLUSIONS AND RECOMMENDATIONS

This computational work models the behavior of Haynes 242 and Hastelloy N in the binary molten salt eutectic mixture KF-$ZrF_4$. Limiting the principal alloying elements to four—nickel, chromium, molybdenum, and iron—allows reasonable conclusions to be made about the nature of the hot corrosion resistance of these materials. It suggests that further alloy composition optimization work could be conducted to further enhance alloy hot corrosion resistance.

The onset of hot corrosion for both alloys is associated with chromium leaching and the formation of $CrF_2$ in relatively mild oxidizing conditions. However, the onset of hot corrosion for Alloy N requires harsher conditions than for Haynes 242. Thermodynamic data for these systems need to be generated in future research efforts in order to get a clearer picture of the mechanisms of hot corrosion onset. First-principles atomistic simulations can illuminate those cases where experimental thermodynamic data is absent.

Another important direction of research is coupling, in real time, the hydrodynamics of molten salt flow inside the reactor with a thermodynamic assessment of corrosion made under the assumption of local equilibrium on a sufficiently fine spatio-temporal grid. This would pave the way to understanding how corrosion develops in real space and time in heat exchanger loop components made of superalloys and steels. Another possible application of this new technology would be the analysis of pyrolytic processes, when molten salts are used for catalytic purposes (e.g., biomass reactors, obtaining quality fuel out of heavy fractions of oil refining, etc.).

In conclusion, continuing this computational research effort will allow nuclear engineers to approach the problem of down selecting materials for NGNP AHTRs with greater confidence, less effort spent on expensive experimental work, and in shorter periods of time.

# 7. Acknowledgments

The author would like to express his sincere gratitude to the managers of the project, Mr. Michael W. "Mike" Patterson and Dr. Michael George McKellar for continuous support of this computational effort. Drs. Piyush Sabharwall and Ali Siahpush and Mr. Denis E. Clark helped to improve the quality of the manuscript by providing their valuable comments and recommendations. Mr. Ronald E. Mizia (retired) has provided his consistent support to our initial efforts to utilize computational thermodynamics of materials at the INL.

# 8. REFERENCES

1. R.E. Thoma and W.R. Grimes, Phase Equilibrium Diagrams For Fused Salt Systems, ORNL Chemistry Division, Technical Report # W-7485-eng-26, June 24 1957. Based on: ANI Quarterly Progress Report June 10, 1952, ORNL-1294, p.91.
2. R.E. Thoma (Editor), Phase Diagrams of Nuclear Reactor Materials, ORNL-2542, November 20, 1959.
3. P. Sabbharwall, E.S. Kim, A. Siahpush, N. Anderson, M.V. Glazoff, B. Phoenix, R.E. Mizia, D.E. Clark, M.G. McKellar, and M.W. Patterson, Feasibility Study of Secondary Heat Exchanger Concepts for Advanced High Temperature Reactor, INL/EXT-11-23076, September 2011.
4. L.C. Olson, Materials Corrosion in Molten LiF-NaF-KF Eutectic Salt, Ph.D Dissertation, University of Wisconsin-Madison, Advisor Prof. Todd R. Allen (2009).
5. L. Olson, J. Ambrosek, K. Sridharan, M. Anderson, T.R. Allen, Materials Corrosion in Molten LiF-NaF-KF salt, Journal of Fluorine Chemistry, vol.130, No. 1, pp.67-73 (2009).
6. ThermoCalc software LLC, public database SSUB4 – a SGTE Substances Database v.4.1.
7. http://cst-www.nrl.navy.mil/lattice/prototype.html.
8. Paul L. Brown, Federico J. Mompean, Jane Perrone, Myriam Illemassène (2005), Chemical thermodynamics of zirconium, Gulf Professional Publishing, p. 144; ISBN 0-444-51803-7.
9. ThermoCalc Classic Version S User's Guide, P. Shi and B. Sundman Editors, ThermoCalc Software AB, Stockholm, Sweden (2010).
10. Anita Magyar, Karbon Szallal Erositett Aluminum Matrixu u Kompositok Al/C Hatareluletenek Jellemzese, Ph.D. Thesis, Miscolc (2004, in Hungarian).
11. G. Hatem, F. Tabaries, and F. Gaune-Escard, Enthalpies de formation des melanges liquides ZrF4-MF (M = Li, Na, K, Rb), Thermochimica Acta, vol. 149, pp.15-26 (1989).
12. G. Hatem, Calculation of Phase Diagrams for the Binary Systems BaF22-KF and KF-ZrF4 and the Ternary System BaF2-KF-ZrF4,Themochimica Acta, vol.260, pp.17-28 (1995).
13. R.A. McDonald, G.C. Sinke, and D.J., Chem. Eng. Data, vol.7, p. 83 (1962).
14. Alekszeeva E.A., Poszipajko V. I.: Diagrams of Melting for Salt Systems ("Diagrammi plavkoszti solevih sisztem") Moscow, Metallurgy Publ. Co. (1977; in Russian).
15. V. Gaumet, M. El-Ghozzi, European J. Solid State Inorg. Chem., vol.34 No.3, pp.283-293 (1997) - crystalline structure of KZrF5.
16. Richard Bornstein, Hans Landolt, Berlin, Springer, 2004. Chapter title: "KZrF5" (2005).

17. V. Dracopoulos, J. Vagelatos and G. N. Papatheodorou, Raman spectroscopic studies of molten ZrF4–KF mixturesand of A2ZrF6, A3ZrF7 (A = Li, K or Cs) compounds J. of Chemical Society, Dalton Transactions, issue 7, pp.1117-1122 (2001).
18. M. M. Godneva, D. L. Motov, N. N. Boroznovskaya, and V. M. Klimkin, Synthesis of Zirconium (Hafnium) Fluoride Compounds and Their X-ray Luminescence Properties, Russian Journal of Inorganic Chemistry, 2007, Vol. 52, No. 5, pp. 661–666. Translated into English by Pleiades Publishing (2007).
19. M.V. Glazov (Glazoff), Phase Equilibria and Calculation of the Thermodynamic Properties Alloys in Binary Systems with Intermediate Superconducting A15-Phases, Ph.D. Thesis (Physical Chemistry) the USSR Academy of Sciences, Moscow Institute of Metallurgy (1987).
20. Hadamard, Jacques, Sur les problèmes aux dérivées partielles et leur signification physique Paris, Gauthier-Villars, pp. 49–52 (1902).
21. Tikhonov, A. N.; Arsenin, V. Y., Solutions of Ill-Posed Problems. New York, Winston (1977).
22. H.L. Lukas, S.G. Fries, and Bo Sundman, Computational Thermodynamics (The CALPHAD Method), Cambridge University Press, Cambridge (2007).
23. Mats Hillert, Phase Equilibria, Phase Diagrams, and Phase Transformations: Their Thermodynamic Basis, 2nd edition, Cambridge University Press, Cambridge (2008).
24. N. Saunders and A.P. Miodownik, CALPHAD – Calculation of Phase Diagrams. A Comprehensive Guide, Pergamon, London (1998).
25. M.I. Temkin, Zhurn. Fiz. Khimii (Russian Journal of Physical Chemistry) vol. 20, no. 1, p. 105 (1946).
26. Zi-Kui Liu, First-Principles calculations and CALPHAD Modeling of Thermodynamics, Journal of Phase equilibria and Diffusion, published online 03 September (2009).
27. Z.-K. Liu, L.Q. Chen, R. Raghavan, Q. Du, J.O. Sofo, S.A. Langer and C. Wolverton, An Integrated Framework for Multi-Scale Materials Simulation and Design, J. of Computer-Aided Mater. Design, vol.11, pp.183-199 (2004).
28. VASP – Vienna Ab initio Simulation Package, http://www.vasp.at/ (2012).
29. M. K. Miller, I. M. Anderson, L. M. Pike and D. L. Klarstrom, Materials Science and Engineering A, v.327, Iss.1, pp. 89-93 (2002).
30. H.E. McCoy, Jr., An Evaluation Of The Molten-Salt Reactor Experiment Hastelloy N Surveillance Specimens - Fourth Group, Report ORNL-TM- 3063, March 1976.
31. Patrice Chartrand and Arthur D. Pelton, Thermodynamic Evaluation and Optimization of the LiF-NaF-KF-MgF2-CaF2 System Using the Modified Quasi-Chemical Model, Met. Mat. Trans A, vol.32A, p.1385 (2001).
32. Vladimir Danielik, Pavel Fellner, and Oldrich Matal, Corrosion of Nickel in the Molten Mixture of LiF-NaF-ZrF4, Acta Chimica Slovaka,vol.2, No.1, pp.3 – 11 (2009).

# Appendix A

# Thermodynamic Data Base for the KF – ZrF4 System

# Appendix A
# Thermodynamic Data Base for the KF – ZrF4 System

```
$ Database file written 01/25/2012
$ Data used from database: SSUB4
 ELEMENT  /-     ELECTRON_GAS                          0.0000E+00   0.0000E+00
0.0000E+00!
 ELEMENT  VA     VACUUM                                0.0000E+00   0.0000E+00
0.0000E+00!
 ELEMENT  F       1/2_MOLE_F2(GAS)                     1.8998E+01   4.4125E+03
1.0134E+02!
 ELEMENT  K      BCC_A2                                3.9098E+01   7.0835E+03
6.4672E+01!
 ELEMENT  ZR     HCP_A3                                9.1224E+01   5.5663E+03
3.9181E+01!

 SPECIES F1K1                         F1K1!
 SPECIES F4ZR1                        F4ZR1!

 FUNCTION   F8809T              2.98150E+02      -583869.251+257.421862*T-
47.79132*T*LN(T)
     -.0046140735*T**2-6.56616E-07*T**3+84928.5*T**(-1);  9.00000E+02  Y
      -566044.318+135.998566*T-32.01124*T*LN(T)-.005759505*T**2
     -1.993335E-06*T**3-2839890*T**(-1);  1.13100E+03  Y
      -603118.731+438.402641*T-71.9648*T*LN(T);  3.00000E+03  N !
 FUNCTION   F9902T              2.98150E+02      -1939125.16+465.509053*T-
81.64412*T*LN(T)
     -.04031231*T**2+3.26213667E-06*T**3+10790.095*T**(-1); 1.18300E+03  Y
      -1974356.84+935.847412*T-150*T*LN(T);  2.00000E+03  N !
$ FUNCTION UN_ASS 298.15 0; 300 N !

 TYPE_DEFINITION % SEQ *!
 DEFINE_SYSTEM_DEFAULT ELEMENT 2 !
 DEFAULT_COMMAND DEF_SYS_ELEMENT VA /- !

Phase LIQUID_SALT % 1 1 !
CONSTITUENT LIQUID_SALT :F1K1,F4ZR1:!
Parameter G(LIQUID_SALT,F1K1;0) 298.15 +F8809T#+27196-24.045977*T;6000 N !
Parameter G(LIQUID_SALT,F4ZR1;0)298.15 +F9902T#+61000-51.5638208*T;6000 N!


 PHASE F1K1_S  %  1  1.0  !
    CONSTITUENT F1K1_S  :F1K1 :  !

   PARAMETER G(F1K1_S,F1K1;0)  2.98150E+02  +F8809T#;   6.00000E+03   N !


 PHASE F4ZR1_S  %  1  1.0  !
    CONSTITUENT F4ZR1_S  :F4ZR1 :  !

   PARAMETER G(F4ZR1_S,F4ZR1;0)  2.98150E+02  +F9902T#;   6.00000E+03  N !
```

# Appendix B

# Thermo-Calc Script used to Compute Metastable KF-ZrF4 phase diagram

# Appendix B
# Thermo-Calc Script used to Compute Metastable KF-ZrF4 phase diagram

```
go data
sw
user
d-sys f k zr
get
go p-3
d-comp f1k1 f4zr1 f
s-co t=1200 p=101325 n=1 x(f4zr1)=0.5 ac(f)=1
c-e
s-a-v 1 x(f4zr1) 0 1
.025
s-a-v 2 t 500 2000
37.5
map
po
s-d-a x m-f f4zr1
s-d-a y t-c
pl
SCREEN
set-inter
```

# Appendix C

# Documented Results of the New Database Performance and the Construction of the KF-ZrF4 Phase Diagram

# Appendix C

# Documented Results of the New Database Performance and the Construction of the KF-ZrF4 Phase Diagram

```
Thermo-Calc version S(build 2532) on Linux 32bit word length
 using compiler: GNU Fortran (GCC) 4.1.2 20080704 (Red Hat 4.1.2-44)
 Copyright (1993,2008) Foundation for Computational Thermodynamics,
 Stockholm, Sweden
 Double precision version linked at 29-06-10 08:34:17
 Only for use at Idaho National Lab
 Local contact Michael Glazoff
SYS: m-f-o
Macro filename: phase_diagram_C.tcm
SYS: THERMODYNAMIC DATABASE module
 Current database: TCS Steels/Fe-Alloys Database v6

 VA  DEFINED
 IONIC_LIQ:Y             L12_FCC                 B2_BCC
 B2_VACANCY              HIGH_SIGMA              DICTRA_FCC_A1
   REJECTED
TDB_TCFE6: Use one of these databases

 TCFE6    = TCS Steels/Fe-Alloys Database v6
 SSUB4    = SGTE Substances Database v4
 SPOT4    = SGTE Potential Database v4
 SALT1    = SGTE Molten Salt Database v1
 ION3     = TCS Ionic Solutions Database v3
 TTNI8    = TT Ni-alloy Database v8
 PURE4    = SGTE Unary (Pure Elements) TDB v4
 PSUB     = TCS Public Pure Substances TDB v1
 PBIN     = TCS Public Binary Alloys TDB v1
 PTERN    = TCS Public Ternary Alloys TDB v1
 PKP      = Kaufman Binary Alloys TDB v1
 PCHAT    = Chatenay-Malabry Binary Alloys TDB v1
 PG35     = G35 Binary Semi-Conductors TDB v1
 PION     = TCS Public Ionic Solutions TDB v2
 PAQ2     = TCS Public Aqueous Soln (SIT) TDB v2
 PAQS2    = TCS Public Aqueous Soln (HKF) TDB v2
 PGEO     = Saxena Pure Minerals Database v1
 MOBNI1   = TCS Ni-Alloys Mobility Database v1
 MOBFE1   =  TCS Fe-Alloys Mobility Database v1
 PFRIB    = Fridberg Dilute Fe-Alloys MDB v1
 USER     = User defined Database

DATABASE NAME /TCFE6/: FILENAME: Current database: User defined Database
This database does not support the DATABASE_INFORMATION command

 VA                      /- DEFINED
TDB_USER: F                       K                       ZR
   DEFINED
TDB_USER: ELEMENTS
 SPECIES
 PHASES
 PARAMETERS
 FUNCTIONS
 -OK
TDB_USER:
```

```
 POLY version  3.32
POLY_3: Normal POLY minimization, not global
 Testing POLY result by global minimization procedure
 Calculated          139  grid points in            0  s
    15 ITS,  CPU TIME USED   0 SECONDS
POLY_3:Increment          /.025/:          POLY_3:Increment          /37.5/:
POLY_3: Version S mapping is selected
 INITIATED WORKSPACES ON FILE RESULT.POLY3
 Generating start equilibrium 1
 Generating start equilibrium 2
 Generating start equilibrium 3
 Generating start equilibrium 4
 Generating start equilibrium 5
 Generating start equilibrium 6
 Generating start equilibrium 7
 Generating start equilibrium 8
 Generating start equilibrium 9
 Generating start equilibrium 10
 Generating start equilibrium 11
 Generating start equilibrium 12

 Organizing start points

Using ADDED start equilibria

 Generating start point   1
 Generating start point   2
 Generating start point   3
 Generating start point   4
 Generating start point   5
 Generating start point   6
 Generating start point   7
 Generating start point   8
 Generating start point   9
 Generating start point 10
 Working hard
 Generating start point 11
 Generating start point 12
 Generating start point 13
 Generating start point 14
 Generating start point 15
 Generating start point 16
 Generating start point 17
 Generating start point 18
 Generating start point 19
 Generating start point 20
 Working hard
 Generating start point 21
 Generating start point 22
 Generating start point 23
 Generating start point 24

 Phase region boundary   1 at:   5.000E-01 5.100E+02
     F1K1_S
  ** F4ZR1_S
 *** Buffer saved on file: RESULT.POLY3
 Calculated..            2 equilibria
 Terminating at axis limit

 Phase region boundary   2 at:   5.000E-01 5.000E+02
     F1K1_S
  ** F4ZR1_S
 Calculated           15 equilibria
```

```
Phase region boundary   3 at:   5.000E-01 9.987E+02
    F1K1_S
 ** F4ZR1_S
 ** LIQUID

Phase region boundary   4 at:   1.592E-01 9.987E+02
    F1K1_S
 ** LIQUID
Calculated           34 equilibria

Phase region boundary   5 at:   6.592E-01 9.987E+02
    F4ZR1_S
 ** LIQUID
Calculated           35 equilibria

Phase region boundary   6 at:   5.000E-01 5.100E+02
    F1K1_S
 ** F4ZR1_S
Calculated           15 equilibria
Terminating at known equilibrium

Phase region boundary   7 at:   5.000E-01 5.100E+02
    F1K1_S
 ** F4ZR1_S
Calculated            2 equilibria
Terminating at known equilibrium
Terminating at axis limit

Phase region boundary   8 at:   5.000E-01 5.100E+02
    F1K1_S
 ** F4ZR1_S
Calculated           15 equilibria
Terminating at known equilibrium

Phase region boundary   9 at:   5.000E-01 5.100E+02
    F1K1_S
 ** F4ZR1_S
Calculated            2 equilibria
Terminating at known equilibrium
Terminating at axis limit

Phase region boundary 10 at:   5.000E-01 5.100E+02
    F1K1_S
 ** F4ZR1_S
Calculated           15 equilibria
Terminating at known equilibrium

Phase region boundary 11 at:   5.000E-01 5.100E+02
    F1K1_S
 ** F4ZR1_S
Calculated..         2 equilibria
Terminating at known equilibrium
Terminating at axis limit

Phase region boundary 12 at:   5.000E-01 5.100E+02
    F1K1_S
 ** F4ZR1_S
Calculated           15 equilibria
Terminating at known equilibrium

Phase region boundary 13 at:   5.000E-01 5.100E+02
    F1K1_S
 ** F4ZR1_S
Calculated            2 equilibria
```

```
Terminating at known equilibrium
Terminating at axis limit

Phase region boundary 14 at:   5.000E-01 5.100E+02
    F1K1_S
 ** F4ZR1_S
Calculated           15 equilibria
Terminating at known equilibrium

Phase region boundary 15 at:   5.000E-01 5.100E+02
    F1K1_S
 ** F4ZR1_S
Calculated            2 equilibria
Terminating at known equilibrium
Terminating at axis limit

Phase region boundary 16 at:   5.000E-01 5.100E+02
    F1K1_S
 ** F4ZR1_S
Calculated           15 equilibria
Terminating at known equilibrium

Phase region boundary 17 at:   1.539E-01 1.003E+03
 ** F1K1_S
    LIQUID
Calculated            2 equilibria
Terminating at known equilibrium

Phase region boundary 18 at:   1.539E-01 1.003E+03
 ** F1K1_S
    LIQUID
Calculated           38 equilibria

Phase region boundary 19 at:   6.647E-01 1.003E+03
 ** F4ZR1_S
    LIQUID
Calculated            2 equilibria
Terminating at known equilibrium

Phase region boundary 20 at:   6.647E-01 1.003E+03
 ** F4ZR1_S
    LIQUID
Calculated           36 equilibria

Phase region boundary 21 at:   5.000E-03 1.127E+03
 ** F1K1_S
    LIQUID
Calculated           15 equilibria

Phase region boundary 22 at:   5.000E-03 1.127E+03
 ** F1K1_S
    LIQUID
Calculated           16 equilibria
Terminating at known equilibrium

Phase region boundary 23 at:   6.683E-01 1.006E+03
 ** F4ZR1_S
    LIQUID
Calculated            2 equilibria
Terminating at known equilibrium

Phase region boundary 24 at:   6.683E-01 1.006E+03
 ** F4ZR1_S
    LIQUID
```

```
 Calculated           24 equilibria

 Phase region boundary 25 at:   8.317E-01 1.110E+03
  ** F4ZR1_S
     LIQUID
 Calculated            9 equilibria
 Terminating at known equilibrium

 Phase region boundary 26 at:   8.317E-01 1.110E+03
  ** F4ZR1_S
     LIQUID
 Calculated           23 equilibria

 Phase region boundary 27 at:   9.950E-01 1.181E+03
  ** F4ZR1_S
     LIQUID
 Calculated           16 equilibria
 Terminating at known equilibrium

 Phase region boundary 28 at:   9.950E-01 1.181E+03
  ** F4ZR1_S
     LIQUID
 Calculated           15 equilibria
 *** BUFFER SAVED ON FILE: RESULT.POLY3
 CPU time for mapping           0 seconds
POLY_3:
  POLY-3 POSTPROCESSOR VERSION 3.2
```

# Appendix D
# Thermo-Calc Script for Modeling of Hot Corrosion of Alloy Haynes 242 in Eutectic Mixture of Molten Salts KF and ZrF4

# Appendix D
# Thermo-Calc Script for Modeling of Hot Corrosion of Hastelloy N in Eutectic Mixture of Molten Salts KF and ZrF4

```
     @@LOGFILE GENERATED ON UNIX / KTH       DATE 2012- 1-23
@@LOGFILE GENERATED ON UNIX / KTH       DATE 2012- 1-23
@@ Testing and debugging of corrosion for alloy N in KF ZrF4

go da
sw
TTNI8
def-sys
ni cr mo fe Zr
rej p laves HCP_A3 NIAL DICTRA_FCC_A1 LIQUID
lis-sys p
get
app
SSUB4
def-sys
ni cr mo fe k f Zr
lis-sys p
rej pha *
res pha gas:g cr1f2_s cr1f2_l cr1f3_s cr1f3_l cr1f4_s
res pha f2fe1_s f2fe1_l f2Ni1_s f2ni1_l f3fe1_s f2fe1_l
res pha f3mo1_s f5mo1_s f5Mo1_l f6mo1_l
lis-sys p
get
append
USER
d-sys f k zr
get
go p-3
def-comp f1k1 f4zr1 f ni cr mo fe
go pol
s-c n=1 p=1e5 t=1013
s-c x(ni)=.355
s-c x(cr)=.036
s-c x(mo)=.084
s-c x(fe)=.025
@@ s-c x(F4Zr1)=0.16
s-c x(F1K1)=0.34
s-c x(f)=1e-11
c-e
l-e

s-c x(f)=1e-12
c-e
l-e

s-c x(f)=1e-13
```

```
c-e

l-e
set-interactive
```

# Appendix E

# The Results of Work of a Thermo-Calc Script Used for Assessment of Hot Corrosion of Hastelloy N in the Eutectic Mixture of Molten Salts KF and ZrF4

# Appendix E
# The Results of Work of a Thermo-Calc Script Used for Assessment of Hot Corrosion of Hastelloy N in the Eutectic Mixture of Molten Salts KF and ZrF4

```
Thermo-Calc version S(build 2532) on Linux 32bit wordlength
 using compiler:GNU Fortran (GCC) 4.1.2 20080704 (Red Hat 4.1.2-44)
 Copyright (1993,2008) Foundation for Computational Thermodynamics,
 Stockholm, Sweden
 Double precision version linked at 29-06-10 08:34:17
 Only for use at Idaho National Lab
 Local contact Michael Glazoff
SYS:m-f-o
Macro filename:: ZRF4_revised_N-PKM.tcm
SYS:SYS:SYS:
SYS: THERMODYNAMIC DATABASE module
 Current database: TCS Steels/Fe-Alloys Database v6

 VA  DEFINED
 IONIC_LIQ:Y             L12_FCC                 B2_BCC
 B2_VACANCY              HIGH_SIGMA              DICTRA_FCC_A1
   REJECTED
TDB_TCFE6: Use one of these databases

 TCFE6    =  TCS Steels/Fe-Alloys Database v6
 SSUB4    =  SGTE Substances Database v4
 SPOT4    =  SGTE Potential Database v4
 SALT1    =  SGTE Molten Salt Database v1
 ION3     =  TCS Ionic Solutions Database v3
 TTNI8    =  TT Ni-alloy Database v8
 PURE4    =  SGTE Unary (Pure Elements) TDB v4
 PSUB     =  TCS Public Pure Substances TDB v1
 PBIN     =  TCS Public Binary Alloys TDB v1
 PTERN    =  TCS Public Ternary Alloys TDB v1
 PKP      =  Kaufman Binary Alloys TDB v1
 PCHAT    =  Chatenay-Malabry Binary Alloys TDB v1
 PG35     =  G35 Binary Semi-Conductors TDB v1
 PION     =  TCS Public Ionic Solutions TDB v2
 PAQ2     =  TCS Public Aqueous Soln (SIT) TDB v2
 PAQS2    =  TCS Public Aqueous Soln (HKF) TDB v2
 PGEO     =  Saxena Pure Minerals Database v1
 MOBNI1   =  TCS Ni-Alloys Mobility Database v1
 MOBFE1   =  TCS Fe-Alloys Mobility Database v1
 PFRIB    =  Fridberg Dilute Fe-Alloys MDB v1
 KFZRF4   =  Molten Salt KF-ZrF4 database
 USER     =  User defined Database

DATABASE NAME /TCFE6/:  Current database: TT Ni-alloy Database v8

 VA  DEFINED
TDB_TTNI8:SPECIES: NI                      CR                      MO
 FE                      ZR  DEFINED
TDB_TTNI8: LAVES                  HCP_A3                  NIAL
 DICTRA_FCC_A1           LIQUID  REJECTED
TDB_TTNI8: GAS:G                    A4B_D1                  BCC_A2
 CR3X_A15                 DELTA                   DELTA_PRIME
 ETA                      FCC_A1                  GAMMA_PRIME
 L10                      MB_ORTH                 MU_PHASE
 NI2M                     NI5M                    NI7M2
 NIMO                     P_PHASE                 R_PHASE
```

```
 SIGMA                    MC                       MN
TDB_TTNI8: REINITIATING GES5 .....
 ELEMENTS .....
 SPECIES ......
 PHASES .......
 PARAMETERS ...
 FUNCTIONS ....
 -OK-
TDB_TTNI8: Use one of these databases

 TCFE6   =  TCS Steels/Fe-Alloys Database v6
 SSUB4   =  SGTE Substances Database v4
 SPOT4   =  SGTE Potential Database v4
 SALT1   =  SGTE Molten Salt Database v1
 ION3    =  TCS Ionic Solutions Database v3
 TTNI8   =  TT Ni-alloy Database v8
 PURE4   =  SGTE Unary (Pure Elements) TDB v4
 PSUB    =  TCS Public Pure Substances TDB v1
 PBIN    =  TCS Public Binary Alloys TDB v1
 PTERN   =  TCS Public Ternary Alloys TDB v1
 PKP     =  Kaufman Binary Alloys TDB v1
 PCHAT   =  Chatenay-Malabry Binary Alloys TDB v1
 PG35    =  G35 Binary Semi-Conductors TDB v1
 PION    =  TCS Public Ionic Solutions TDB v2
 PAQ2    =  TCS Public Aqueous Soln (SIT) TDB v2
 PAQS2   =  TCS Public Aqueous Soln (HKF) TDB v2
 PGEO    =  Saxena Pure Minerals Database v1
 MOBNI1  =  TCS Ni-Alloys Mobility Database v1
 MOBFE1  =  TCS Fe-Alloys Mobility Database v1
 PFRIB   =  Fridberg Dilute Fe-Alloys MDB v1
 KFZRF4  =  Molten Salt KF-ZrF4 database
 USER    =  User defined Database

DATABASE NAME /TTNI8/:  Current database: SGTE Substances Database v4

 VA  DEFINED
APP:ELEMENTS: NI                        CR                        MO
 FE                      K                         F
 ZR  DEFINED
APP: GAS:G                    CR_S                      CR_L
 CR1F2_S                  CR1F2_L                   CR1F3_S
 CR1F3_L                  CR1F4_S                   F1K1_S
 F1K1_L                   F2FE1_S                   F2FE1_L
 F2NI1_S                  F2NI1_L                   F2ZR1_S
 F2ZR1_L                  F3FE1_S                   F3FE1_L
 F3MO1_S                  F3ZR1_S                   F3ZR1_L
 F4ZR1_S                  F4ZR1_L                   F5MO1_S
 F5MO1_L                  F6MO1_L                   FE_S
 FE_S2                    FE_S3                     FE_L
 FE3MO2_S                 K_S                       K_L
 MO_S                     MO_L                      NI_S
 NI_L                     ZR_S                      ZR_S2
 ZR_L
APP: GAS:G                    CR_S                      CR_L
 CR1F2_S                  CR1F2_L                   CR1F3_S
 CR1F3_L                  CR1F4_S                   F1K1_S
 F1K1_L                   F2FE1_S                   F2FE1_L
 F2NI1_S                  F2NI1_L                   F2ZR1_S
 F2ZR1_L                  F3FE1_S                   F3FE1_L
 F3MO1_S                  F3ZR1_S                   F3ZR1_L
 F4ZR1_S                  F4ZR1_L                   F5MO1_S
 F5MO1_L                  F6MO1_L                   FE_S
 FE_S2                    FE_S3                     FE_L
 FE3MO2_S                 K_S                       K_L
```

```
 MO_S                    MO_L                    NI_S
 NI_L                    ZR_S                    ZR_S2
 ZR_L  REJECTED
APP: GAS:G                   CR1F2_S                 CR1F2_L
 CR1F3_S                 CR1F3_L                 CR1F4_S
   RESTORED
APP: F2FE1_S                 F2FE1_L                 F2NI1_S
 F2NI1_L                 F3FE1_S  RESTORED
APP: F3MO1_S                 F5MO1_S                 F5MO1_L
 F6MO1_L  RESTORED
APP: GAS:G                    CR1F2_S                   CR1F2_L
 CR1F3_S                  CR1F3_L                  CR1F4_S
 F2FE1_S                  F2FE1_L                  F2NI1_S
 F2NI1_L                  F3FE1_S                  F3MO1_S
 F5MO1_S                  F5MO1_L                  F6MO1_L
APP: ELEMENTS .....
 SPECIES ......
 PHASES .......
 PARAMETERS ...
 FUNCTIONS ....

 List of references for assessed data

   CR1F2 T.C.R.A.S. Class: 7
      CHROMIUM DIFLUORIDE
   CR1F3 T.C.R.A.S. Class: 7
      Data refitted by IA
   CR1F4 I. BARIN 3rd. Edition
      CHROMIUM TETRAFLUORIDE. H298 modified.
   F2FE1 T.C.R.A.S Class: 6
      Data provided by T.C.R.A.S. October 1996
   F2NI1 T.C.R.A.S Class: 5
      Data provided by T.C.R.A.S. October 1996
   F3FE1 T.C.R.A.S Class: 6
      Data provided by T.C.R.A.S. October 1996
      Phase transitions of the second order
      (of the antiferromagnetic-paramagnetic type) considered at 367K.
      Cp smoothed again to represent better the second transition (IA).
   F3MO1 T.C.R.A.S. Class: 7
   F5MO1 T.C.R.A.S. Class: 7
   F6MO1 T.C.R.A.S. Class: 5
 -OK-
APP: Use one of these databases

 TCFE6   =  TCS Steels/Fe-Alloys Database v6
 SSUB4   =  SGTE Substances Database v4
 SPOT4   =  SGTE Potential Database v4
 SALT1   =  SGTE Molten Salt Database v1
 ION3    =  TCS Ionic Solutions Database v3
 TTNI8   =  TT Ni-alloy Database v8
 PURE4   =  SGTE Unary (Pure Elements) TDB v4
 PSUB    =  TCS Public Pure Substances TDB v1
 PBIN    =  TCS Public Binary Alloys TDB v1
 PTERN   =  TCS Public Ternary Alloys TDB v1
 PKP     =  Kaufman Binary Alloys TDB v1
 PCHAT   =  Chatenay-Malabry Binary Alloys TDB v1
 PG35    =  G35 Binary Semi-Conductors TDB v1
 PION    =  TCS Public Ionic Solutions TDB v2
 PAQ2    =  TCS Public Aqueous Soln (SIT) TDB v2
 PAQS2   =  TCS Public Aqueous Soln (HKF) TDB v2
 PGEO    =  Saxena Pure Minerals Database v1
 MOBNI1  =  TCS Ni-Alloys Mobility Database v1
 MOBFE1  =  TCS Fe-Alloys Mobility Database v1
 PFRIB   =  Fridberg Dilute Fe-Alloys MDB v1
```

```
 KFZRF4  =  Molten Salt KF-ZrF4 database
 USER    =  User defined Database

DATABASE NAME /SSUB4/:  Current database: Molten Salt KF-ZrF4 database
This database does not support the DATABASE_INFORMATION command

 VA                      /-  DEFINED
APP: F                       K                        ZR
   DEFINED
APP:APP:APP: ELEMENTS .....
 SPECIES ......
 PHASES .......
 PARAMETERS ...
 FUNCTIONS ....
 -OK-
APP:
 POLY version  3.32
Using global minimization procedure
 Calculated        25511  grid points in            0  s
 Found the set of lowest grid points in             0  s
 Calculated POLY solution       1 s, total time     1  s
POLY_3:Output file: /SCREEN/:
Options /VWCS/:
 Output from POLY-3, equilibrium =     1, label A0  , database: SSUB4

 Conditions:
 N=1, P=1E5, T=1013, X(NI)=0.355, X(CR)=3.6E-2, X(MO)=8.4E-2,
X(FE)=2.5E-2,
    X(F1K1)=0.34, X(F)=1E-11
 DEGREES OF FREEDOM 0

 Temperature   1013.00 K (   739.85 C),  Pressure  1.000000E+05
 Number of moles of components  1.00000E+00,  Mass in grams  7.86685E+01
 Total Gibbs energy -5.83585E+05,  Enthalpy -4.41174E+05,  Volume0.00000E+00

 Component               Moles       W-Fraction  Activity  Potential Ref.stat
 F1K1                    3.4000E-01  2.5109E-01 5.8566E-35 -6.6389E+05 SER
 F4ZR1                   1.6000E-01  3.4008E-01 6.516E-108 -2.0787E+06 SER
 F                       6.9221E-12  1.6716E-12 1.4151E-22 -4.2374E+05 SER
 NI                      3.5500E-01  2.6484E-01 2.8025E-03 -4.9502E+04 SER
 CR                      3.6000E-02  2.3794E-02 6.8151E-04 -6.1411E+04 SER
 MO                      8.4000E-02  1.0244E-01 4.9171E-03 -4.4766E+04 SER
 FE                      2.5000E-02  1.7748E-02 2.8521E-04 -6.8748E+04 SER

 LIQUID_SALT                 Status ENTERED     Driving force  0.0000E+00
 Moles 5.0000E-01, Mass 4.6507E+01, Volume fraction 0.0000E+00 Massfractions:
 F4ZR1  5.75272E-01  MO     0.00000E+00  NI     0.00000E+00  FE0.00000E+00
 F1K1   4.24728E-01  CR     0.00000E+00  F      0.00000E+00

 FCC_A1                      Status ENTERED     Driving force  0.0000E+00
 Moles 4.2158E-01, Mass 2.6301E+01, Volume fraction 0.0000E+00 Massfractions:
 NI     7.16516E-01  CR     5.74514E-02  F4ZR1  2.68027E-12  F-1.21809E-12
 MO     1.77947E-01  FE     4.80855E-02  F1K1   0.00000E+00

 MU_PHASE                    Status ENTERED     Driving force  0.0000E+00
 Moles 7.8417E-02, Mass 5.8610E+00, Volume fraction 0.0000E+00 Massfractions:
 MO     5.76486E-01  CR     6.15645E-02  F1K1   0.00000E+00  F4ZR10.00000E+00
 NI     3.39516E-01  FE     2.24332E-02  F      0.00000E+00

 CR1F2_S                     Status ENTERED     Driving force  0.0000E+00
 Moles 1.2913E-11, Mass 3.8734E-10, Volume fraction 0.0000E+00  Mass
fractions:
 CR     5.77785E-01  F1K1   0.00000E+00  NI     0.00000E+00  F4ZR10.00000E+00
 F      4.22215E-01  MO     0.00000E+00  FE     0.00000E+00
```

```
POLY_3:POLY_3: Using global minimization procedure
 Using already calculated grid
 Found the set of lowest grid points in             0  s
 Calculated POLY solution       0 s, total time     0  s
POLY_3:Output file: /SCREEN/:
Options /VWCS/:
 Output from POLY-3, equilibrium =     1, label A0  , database: SSUB4

 Conditions:
 N=1, P=1E5, T=1013, X(NI)=0.355, X(CR)=3.6E-2, X(MO)=8.4E-2,
X(FE)=2.5E-2,
    X(F1K1)=0.34, X(F)=1E-12
 DEGREES OF FREEDOM 0

 Temperature   1013.00 K (   739.85 C),  Pressure  1.000000E+05
 Number of moles of components  1.00000E+00,  Mass in grams  7.86685E+01
 Total Gibbs energy -5.83585E+05,  Enthalpy -4.41174E+05,  Volume0.00000E+00

 Component               Moles       W-Fraction  Activity  Potential Ref.stat
 F1K1                    3.4000E-01  2.5109E-01 5.8566E-35 -6.6389E+05 SER
 F4ZR1                   1.6000E-01  3.4008E-01 6.516E-108 -2.0787E+06 SER
 F                      -1.6863E-12 -4.0724E-13 1.3353E-22 -4.2423E+05 SER
 NI                      3.5500E-01  2.6484E-01 2.8025E-03 -4.9502E+04 SER
 CR                      3.6000E-02  2.3794E-02 6.8151E-04 -6.1411E+04 SER
 MO                      8.4000E-02  1.0244E-01 4.9171E-03 -4.4766E+04 SER
 FE                      2.5000E-02  1.7748E-02 2.8521E-04 -6.8748E+04 SER

 LIQUID_SALT                  Status ENTERED     Driving force  0.0000E+00
 Moles 5.0000E-01, Mass 4.6507E+01, Volume fraction 0.0000E+00 Massfractions
 F4ZR1  5.75272E-01  MO     0.00000E+00  NI     0.00000E+00  FE0.00000E+00
 F1K1   4.24728E-01  CR     0.00000E+00  F      0.00000E+00

 FCC_A1                       Status ENTERED     Driving force  0.0000E+00
 Moles 4.2158E-01, Mass 2.6301E+01, Volume fraction 0.0000E+00 Massfractions:
 NI     7.16516E-01  CR     5.74514E-02  F4ZR1  2.68027E-12  F-1.21809E-12
 MO     1.77947E-01  FE     4.80855E-02  F1K1   0.00000E+00

 MU_PHASE                     Status ENTERED     Driving force  0.0000E+00
 Moles 7.8417E-02, Mass 5.8610E+00, Volume fraction 0.0000E+00 Massfractions:
 MO     5.76486E-01  CR     6.15645E-02  F1K1   0.00000E+00  F4ZR10.00000E+00
 NI     3.39516E-01  FE     2.24332E-02  F      0.00000E+00

POLY_3:POLY_3: Using global minimization procedure
 Using already calculated grid
 Found the set of lowest grid points in             0  s
 Calculated POLY solution       0 s, total time     0  s
Options /VWCS/:
 Output from POLY-3, equilibrium =     1, label A0  , database: SSUB4

 Conditions:
 N=1, P=1E5, T=1013, X(NI)=0.355, X(CR)=3.6E-2, X(MO)=8.4E-2,
X(FE)=2.5E-2,
    X(F1K1)=0.34, X(F)=1E-13
 DEGREES OF FREEDOM 0

 Temperature   1013.00 K (   739.85 C),  Pressure  1.000000E+05
 Number of moles of components  1.00000E+00,  Mass in grams  7.86685E+01
 Total Gibbs energy -5.83585E+05,  Enthalpy -4.41174E+05,  Volume 0.00000E+00

 Component               Moles       W-Fraction  Activity  Potential Ref.stat
 F1K1                    3.4000E-01  2.5109E-01 5.8566E-35 -6.6389E+05 SER
 F4ZR1                   1.6000E-01  3.4008E-01 6.516E-108 -2.0787E+06 SER
 F                      -1.6863E-12 -4.0724E-13 1.1685E-22 -4.2535E+05 SER
```

```
NI                      3.5500E-01  2.6484E-01 2.8025E-03 -4.9502E+04 SER
CR                      3.6000E-02  2.3794E-02 6.8151E-04 -6.1411E+04 SER
MO                      8.4000E-02  1.0244E-01 4.9171E-03 -4.4766E+04 SER
FE                      2.5000E-02  1.7748E-02 2.8521E-04 -6.8748E+04 SER

LIQUID_SALT                 Status ENTERED     Driving force 0.0000E+00
Moles 5.0000E-01, Mass 4.6507E+01, Volume fraction 0.0000E+00 Massfractions:
F4ZR1  5.75272E-01  MO     0.00000E+00  NI     0.00000E+00  FE0.00000E+00
F1K1   4.24728E-01  CR     0.00000E+00  F      0.00000E+00

FCC_A1                      Status ENTERED     Driving force  0.0000E+00
Moles 4.2158E-01, Mass 2.6301E+01, Volume fraction 0.0000E+00 Massfractions:
NI     7.16516E-01  CR     5.74514E-02  F4ZR1  2.68027E-12  F-1.21809E-12
MO     1.77947E-01  FE     4.80855E-02  F1K1   0.00000E+00

MU_PHASE                    Status ENTERED     Driving force  0.0000E+00
Moles 7.8417E-02, Mass 5.8610E+00, Volume fraction 0.0000E+00 Massfractions:
MO     5.76486E-01  CR     6.15645E-02  F1K1   0.00000E+00  F4ZR10.00000E+00
NI     3.39516E-01  FE     2.24332E-02  F      0.00000E+00
```